1   Regional Assessment and Uncertainty Analysis of Carbon and Nitrogen Balances at
2   cropland scale using the ecosystem model LandscapeDNDC

4   Odysseas Sifounakis[1], Edwin Haas[2], Klaus Butterbach-Bahl[2,3] and Maria P. Papadopoulou[1]

6   [1] Laboratory of Physical Geography and Environmental Impacts, School of Rural, Surveying
7   and Geoinformatics Engineering, National Technical University of Athens, Athens, 15780,
8   Greece

9   [2] Institute of Meteorology and Climate Research (IMK-IFU), Karlsruhe Institute of Technology,
10   Kreuzeckbahnstr. 19, D-82467 Garmisch-Partenkirchen, Germany

11   [3] Department of Agroecology - Center for Landscape Research in Sustainable Agricultural
12   Futures - Land-CRAFT, Aarhus University, Aarhus, 8000, Denmark

13   *Correspondence to*: Edwin Haas (edwin.haas@kit.edu)

15   Abstract

16   The assessment of cropland carbon and nitrogen (C & N) balances play a key role to identify

17   cost effective mitigation measures to combat climate change and reduce environmental

18   pollution. In this paper, a biogeochemical modelling approach is adopted to assess all C & N

19   fluxes in a regional cropland ecosystem of Thessaly, Greece. Additionally, the estimation and

20   quantification of the modelling uncertainty in the regional inventory are realized through the

21   propagation of parameter distributions through the model leading to result distributions for

22   modelling estimations. The model was applied on a regional dataset of approximately 1000

23   polygons deploying model initializations and crop rotations for the 5 major crop cultivations

24   and for a timespan of 8 years. The full statistical analysis on modelling results (including the

25   uncertainty ranges given as $\pm$ values) yields for the C balance carbon input fluxes into the soil

26   of 12.4 ± 1.4 tons C ha^{-1} yr^{-1} and output fluxes of 11.9 ± 1.3 tons C ha^{-1} yr^{-1}, with a resulting

27   average carbon sequestration of 0.5 ± 0.3 tons C ha^{-1} yr^{-1}. The averaged N influx was $212.3 \pm$

28   9.1 kg N ha^{-1} yr^{-1} while outfluxes were estimated on average of 198.3 ± 11.2 kg N ha^{-1} yr^{-1}. The

29   net N accumulation into the soil nitrogen pools was estimated to 14.0 ± 2.1 kg N ha^{-1} yr^{-1}. The

30   N outflux consist of gaseous N fluxes composed by N_2O emissions 2.6 ± 0.8 kg N_2O-N ha^{-1} yr^{-}

31   ^{1}, NO emissions of 3.2 ± 1.5 kg NO-N ha^{-1} yr^{-1}, N_2 emissions 15.5 ± 7.0 kg N_2-N ha^{-1} yr^{-1} and

32   NH_3 emissions of 34.0 ± 6.7 kg NH_3-N ha^{-1} yr^{-1}, as well as aquatic N fluxes (only nitrate leaching

33   into surface waters) of 14.1 ± 4.5 kg NO_3-N ha^{-1} yr^{-1}, N fluxes of N removed from the fields in

34   yields, straw and feed of 128.8 ± 8.5 kg N ha^{-1} yr^{-1}.

36   KEYWORDS: greenhouse emissions, ecosystem modelling, cropland carbon and nitrogen

37   balance, inventory, Thessaly region, LandscapeDNDC

40   Graphical abstract: Result distributions of all nitrogen fluxes with means and medians
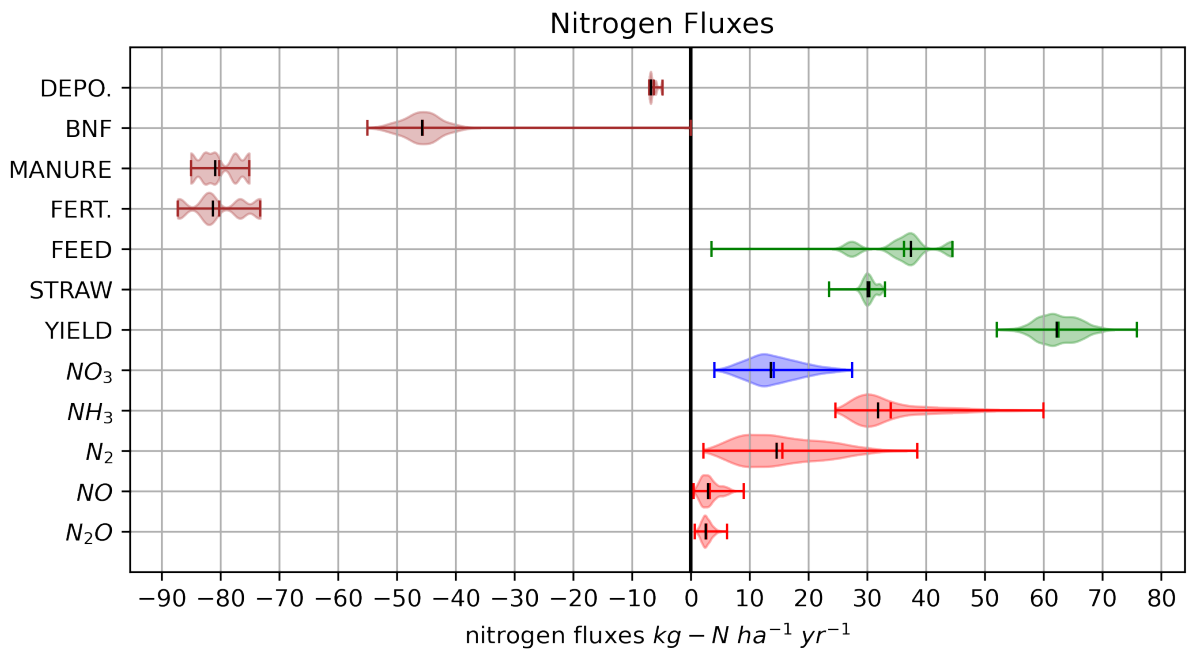
1 Introduction

Food security as well as the agricultural productivity depend to a major extend on the applied nitrogen (N) fertilizers (Klatt et al., 2015a). Worldwide, the N fertilizer use for the years 1960 to 2005 has increased from 30 to 154 million tons (IFADATA, 2015). In Europe, the increase of yields in arable land and grassland systems was 45-70% since 1950 (EFMA, 2009) due to the agricultural production systems intensification. Excessive use of N fertilizers, though beneficially affecting the yield, could cause a harmful impact to the environment, e.g. increased gaseous emissions and aquatic fluxes of nitrous oxide (N_2O) to the atmosphere and leaching of nitrate (NO_3) into water bodies (Erisman et al., 2011; Galloway et al., 2013; Kim et al., 2015) The N_2O poses a twofold environmental threat. From the one hand, it is a strong greenhouse gas with a warming potential of 300 times greater (in a 100-year time period) than carbon dioxide (CO_2) and from the other hand, it is a major driver of ozone depletion in stratosphere (Ravishankara et al., 2009). The fertilizer use aiming at the increase of the agricultural production is the most crucial anthropogenic source of atmospheric N_2O, which at present contributes for approximately 45% of total anthropogenic N_2O emissions on a global scale (Jones et al., 2014). Because of the global population growth and thus a growing food and feed demand (Godfray et al., 2010), the fertilizer use will probably increase. Consequently, the prediction of the current business-as-usual scenarios show doubled anthropogenic N_2O emissions by the year 2050 (Davidson and Kanter, 2014). The European countries have recently set up bilateral agreements in order to reduce N_2O emissions from cultivated crop lands (EU-Commission, 2014). Similarly, the European Nitrates Directive (EU-Commission, 2019; Musacchio et al., 2020) aims at NO_3 leaching reduction to water bodies to avoid both an increase of eutrophication (Camargo and Alonso, 2006) and drinking water pollution. Because of the hazardous N_2O and NO_3 effects, agricultural systems are necessary to be evaluated for their profitability and productivity as well as for their impacts to the environment.

The N_2O and NO_3 production and consumption in agricultural lands are regulated to a large extend by N plant uptake and, also, the microbial processes of denitrification and nitrification (Butterbach-Bahl et al., 2013). The factors controlling both the microbial metabolism and plant

72 N uptake are a) soil conditions (Butterbach-Bahl et al., 2013) and b) cultivation management

73 practices e.g. crop rotation, fertilizing amount and timing, and ploughing (Smith et al., 2008).

74 In order to reach a minimization of the environmental footprint of agricultural production while

75 securing the global food security (Garnett et al., 2013), it is mandatory to tighten the N cycling

76 on intensified agricultural systems e.g., by harmonizing N demand of crops with soil N

77 availability by N fertilization.

78 Full nitrogen balance inventories provide a comprehensive understanding of the different N

79 input and output fluxes within an arable system to the scientific community, farmers and policy

80 makers. The assessment of the N balance is essential to optimize nitrogen use and production

81 and minimize environmental impact and pollution. Especially policy making and regulatory

82 bodies require accurate and robust information on all different nitrogen fluxes to develop

83 effective strategies in agricultural N management. Up to now, our understanding of N cycling

84 in arable land lacks observations of the full N balance as only few studies tried to quantify the

85 total N balance of agricultural systems, e.g. (Zistl-Schlingmann et al., 2020) using stable

86 isotope techniques or (Schroeck et al., 2019) using process based modelling.

87 A recent opinion paper by a large group of leading scientists Grosz et al., (2023) in the field of

88 process based ecosystem modelling identified the lack of knowledge on the full N balance and

89 "the scarcity of complete modeled N balances in the literature stems from the reluctance of the

90 scientific community to support the publication of unvalidated modeled results, especially given

91 that the simulation results of these neglected N pools and fluxes may be unrealistic. This this

92 self-censorship of authors has resulted in a missed opportunity to share knowledge and

93 improve our understanding of modeled processes."

94 Grosz et al., (2023) conclude that "including the entire N balance and related should become

95 standard when publishing the results of N model studies." Grosz et al., (2023) emphasize that

96 this would allow to assess the robustness of modelled N fluxes and full N balances, and to

97 illustrate the diversity and uncertainty of the different process based modeling approaches,

98 e.g. modelling denitrification processes in soils.

99   In this analysis, the process-based bio-geochemical model LandscapeDNDC (Haas et al.,

100   2013) was applied to the agricultural cropland systems in the region of Thessaly (Greece). The

101   objective of our study was threefold:

102   i)   Assesing and reporting the cropland C and N balance including all associated

103   fluxes such as e.g. CO_2, N_2O and NH_3 emissions, NO_3 leaching as well as the soil

104   carbon stock changes as demanded by Grosz et al., (2023).

105   ii)   Increasing the robustness and trustworthiness of the balance modelling by

106   assesing and quantifying the modelling uncertainty of the simulated C and N

107   balance and flux estimations as requested before by the IPCC (IPCC, 2019)

108   iii) Presenting a regional uncertainty assessment methodology for C and N cycling to

109   advance the balance modelling by propagating 500 joint parameter and input data

110   distributions through the model (each representing a full regional C and N balance

111   inventory simulation) yielding regional result distributions for any modelling

112   estimations.

113

114   2   Material and Methods

115   2.1   Model description

116   LandscapeDNDC is a modular process-based ecosystem model for simulating the bio-

117   geochemical change of C and N in croplands, forest and grassland systems at both site and

118   regional scale. The modules combined are about plant growth, micro-meteorology, water

119   cycling, physico-chemical-plant and microbial C and N cycling and exchange processes with

120   atmosphere and hydrosphere of terrestrial ecosystems. LandscapeDNDC is a generality of the

121   plant development and soil biogeochemistry of the agricultural DNDC and Forest-DNDC (Li,

122   2000). There is a successful application of earlier model versions in a number of studies, e.g.

123   water balance (Grote et al., 2009; Holst et al., 2010), plant growth (Cameron et al., 2013;

124   Werner et al., 2012), NO_3 leaching (Kim et al., 2015; Thomas et al., 2016) and soil respiration

125   and gas emission trace (Chirinda et al., 2011; Kraus et al., 2014; Molina-Herrera et al., 2015).

126 For the initialization of LandscapeDNDC physical and chemical site-specific soil profile

127 information is used (specified for different soil depths): Soil organic carbon (SOC) and nitrogen

128 (SON) content, soil texture (clay, sand and silt content), of the plant growth and soil

129 biogeochemistry, bulk density, pH value, saturated hydraulic conductivity, field capacity and

130 wilting point. Daily or hourly climate data of air temperature (max, min and average), N

131 deposition, precipitation, and atmospheric CO_2 concentration are used in LandscapeDNDC in

132 combination with agricultural management practices e.g. crop planting and harvesting,

133 fertilizing (synthetic and organic) or feed cutting and tilling are used to drive LandscapeDNDC

134 simulations. Regarding fertilization management three types of mineral fertilizers, i.e. urea,

135 compound fertilizers based on NH_4 and NO_3 as well as organic amendments, i.e. green

136 manure, farmyard manure, slurry, straw, bean cake and compost are currently considered.

137 The growth of crops and grasses is similar to the DNDC approach using two major parameters

138 that describe seasonal plant development (cumulative temperature degrees days) and

139 maximum reachable biomass under optimum conditions (Li, 2000) while daily growth

140 limitations due to water and nutrient availability are considered. Model parameters describing

141 soil and vegetation characteristics are obtained from an external parameter library. In

142 LandscapeDNDC, the parameterization of the main cultivated commodity crops in Europe

143 occurs by default parameter sets representing an average plant type while process parameter

144 values for micro-meteorology, water cycle and bio-geochemical processes were obtained from

145 previous validation studies, e.g. (Klatt et al., 2015a; Molina-Herrera et al., 2016; Rahn et al.,

146 2012) proving that the LandscapeDNDC model could be universally applicable for similar

147 conditions.

148 For all simulations in the current study, site-specific crop parameterizations were derived in a

149 preceding analysis of various site scale simulations and validations of yield characteristics

150 across the region. An overview of the crops cultivated at the different study sites and detailed

151 information on specific crop rotations used to simulate crop growth are provided in Table A2

152 (supplementary material).

2.2 Case study description and input data

The region of Thessaly is located in Central Greece covering a total area of 14 000 Km^2, where 5000 Km^2 is lowland and approx. 2300 Km^2 and 6500 Km^2 are semi-mountainous and mountainous land respectively. The plain of Thessaly is considered to be among the largest agricultural land of the country (Kalivas et al., 2001) accounting for almost 410 000 ha, of which about 370 000 ha is arable land where almost 80% is covered by annual and 10% by perennial crops (ELSTAT, 2012). The crop/plant production of the region is around 14.2% (ELSTAT, 2012) of the total production of the country (2nd in Greece).

Soil input data for the region was available from the European Project Nitro Europe IP (Sutton et al., 2013) based on the European Soil Database (ESDB v2.0, 2004) containing, soil type and soil profile description of bulk density, SOC content, texture (sand, silt clay), pH value, stone fraction, saturated hydraulic conductivity, wilting point and water-holding capacity in various soil strata (Cameron et al., 2013). A regional soil dataset for the area of interest contained about 1500 spatial polygons out of which approximately 1000 covered the cultivated cropland that was finally simulated. The climate data for the regional simulations was derived at polygon level from gridded ERA5 climate data for Greece.

2.3 Agricultural Management and model input data processing

The total cultivated area and the respective yields for the years 2010 to 2016, used in the current analysis were obtained from the Hellenic Statistical Authority (ELSTAT). Moreover, data associated with the animal capital for the respective years was also provided (ELSTAT) in order to estimate the annual manure production distributed in the region however no data is available on whether and how much of the manure is used in croplands. For the water management, the percentage of irrigated and non-irrigated land (estimated to almost 50% for each case) was also given (ELSTAT) while indicative sets of irrigation management data were acquired through the River Basin Management Plans of the Special Secretariat for Water, Ministry of Environment and Energy (YPEKA, Portmann et al., 2010). The irrigation water volumes were estimated based on the crops needs and the minimum and maximum quantities

180   necessary according to literature while using upscaling tools to get the regional values. The

181   fertilization data sets were provided by Fertilizer Producers and Merchandiser Association

182   (FPMA) for the recent years (2010-2016) and are equated to the annual consumed quantities

183   on a national level, scaled down to a regional level based on crop pattern in the Region of

184   Thessaly cultivated land.

185   In this study, the five main crops maize, wheat, clover, cotton and barley were considered,

186   covering the majority of the cultivated arable land in the region (over 95%) while the remaining

187   cropland was included acquiring the final corrected land/crop coverage. In Table 1 the resulting

188   crop rotation scenarios (R1 - R5) are presented for the evaluation period 2012 - 2016. Note,

189   each rotation sequence (R1 – R5) is shifted in time such that for each year, each crop appears

190   exactly in one rotation. Based on the crop cover contribution in each simulated year the crop

191   rotation contribution factors were estimated and are summarized in Table 2. The management

192   practices were based on the general agricultural practices applied in the region and information

193   provided by farmers.

194

195   *Table 1. Summary of the crop rotation scenarios (R1- R5) for the region of Thessaly. The crop abbreviations corn,*
196   *wiwh, clover, cott and wbar refer to maize (food corn and silage maize), winter wheat, clover (legume feed crops*
197   *s.a. alfalfa or vetch), cotton and winter barley respectively.*

year	R1	R2	R3	R4	R5
2012	clover	cotton	wbar	corn	wiwh
2013	cotton	wbar	corn	wiwh	clover
2014	wbar	corn	wiwh	clover	cotton
2015	corn	wiwh	clover	cotton	wbar
2016	wiwh	clover	cotton	wbar	corn

198

199   *Table 2. Crop cultivation area contribution per year to the aggregation of the five rotations; data constant across*
200   *the region of Thessaly*

Crop Rotation Contribution [% / 100]					
Years	R1	R2	R3	R4	R5
2012	0.15	0.15	0.45	0.11	0.14
2013	0.13	0.29	0.09	0.10	0.39

2014	0.29	0.13	0.10	0.35	0.12
2015	0.15	0.11	0.43	0.16	0.16
2016	0.10	0.36	0.14	0.14	0.25

201

202

2.4 Uncertainty analysis

204 As stated in the IPCC 2006 guidelines and updated in 2019, the assessment of uncertainty is

205 considered a major and crucial/mandatory component when compiling regional or national

206 GHG emission inventories (Larocque et al., 2008). The difference in scale in which the model

207 is used results in divergent errors of the C and N dynamics prediction across different climate

208 zones and scales. Thus, uncertainty analysis is a crucial step towards a higher quality decision

209 making process. The sources of uncertainty can vary and are related to a) the initial conditions

210 (starting values), b) the drivers (e.g. climate and crop management data), c) the conceptual

211 model uncertainty and d) the parameter uncertainty of the various processes (Refsgaard et al.,

212 2007; Wang and Chen, 2012).

213 Santabárbara, (2019) performed a Bayesian Model Calibration and Uncertainty Analysis using

214 a Monte Carlo Markov Chain (MCMC) approach targeting uncertainties associated to the data

215 (bulk density, SOC, pH, clay content) of the initial soil conditions, drivers (cropland

216 management such as fertilization/manure rates & timing, harvest & seeding timing, tillage

217 timing) and bio-geochemical process parameterizations.

218 In order to identify the most sensitive process parameters with a reduced number of model

219 simulations, the Morris method (Morris, 1991) obtains a hierarchy of parameters influence on

220 a given output (gaseous N fluxes) and evaluates whether a non-linearity exists or not. (Morris,

221 1991) proposed that this order can be assessed through the statistical analysis of the changes

222 in the model output, produced by the "one-step-at-a-time" changes in "n" number of proposed

223 parameters. Incremental steps of each parameter range, lead to identifying which ones have

224 substantial influences over the concerned results, without neglecting that some effects could

225   cancel each other (Saltelli et al., 2000), leading to the identification of the 24 most sensitive

226   process parameters (Houska et al., 2017; Myrgiotis et al., 2018b).

227

228   Metropolis – Hastings algorithm

229   The Markov Chain Monte Carlo (MCMC) Metropolis–Hastings algorithm results in numerous

230   parameter sets that approximate the posterior joint parameter distribution by performing a

231   random walk through the space of joint parameter values. This probability evaluation of the

232   data obtained from each step leads to the update of the initial uniform parameter distributions.

233   Bayes' formula relating conditional probabilities may become a powerful and practical

234   computational tool when combined with Markov chain processes and Monte Carlo methods,

235   so-called Markov Chain Monte Carlo (MCMC). A Markov chain is a special type of discrete

236   stochastic processes wherein the probability of an event depends only on the event that

237   immediately precedes it. Integrating parameters (θ) and observation data (D) into Bayes' rule

238   results in the formula:

239

$$P(\theta|D) = \frac{P(D \mid \theta) * P(\theta)}{P(D)} \qquad \textit{2.1}$$

240   where $P(D \mid \theta)$, the probability of the data, is used to obtain the probability of these parameters

241   updated by the data: $P(\theta|D)$ where the evidence is computed as:

242

$$P(D) = \int likelyhood \cdot prior \cdot d\theta \qquad \textit{2.2}$$

243   where $P(D)$ can be numerically approximated with the aforementioned MCMC method (Robert

244   and Casella, 2011).

245   The method uses prior knowledge concerning the sources of the model uncertainty to obtain

246   a narrowed posterior distribution for each one of the sources. By propagating the parameter

247   distributions through the model, the overall uncertainty in the model results can be quantified.

248 In a previous study by Santabárbara, (2019), an extensive sensitivity analysis on all soil bio-

249 geochemical process parameters, soil initial data and arable management data was performed

250 identifying the 24 most sensitive process parameters (listed in supplementary material), the

251 most sensitive soil initial data (soil profile data on bulk density, soil organic carbon content, pH

252 value) and the most sensitive management information (fertilization and manure N rates, tilling

253 depth) to aquatic and gaseous N fluxes from arable soils. This was digested in the MCMC

254 simulation sampling a combination of 24 parameter values, 3 values of soil initial data and 3

255 management information. The sampling of the soil initial data as well as the management data

256 was performed as perturbations to the existing data: For each quantity, a perturbation was

257 sampled individually and applied to all corresponding values in the soil profile or to all years in

258 the management description. The MCMC simulation performed by Santabárbara, (2019)

259 simulated more than 100 000 iterations for various arable sites until the MCMC simulation

260 converged towards a stable combined posterior distribution of parameter values and soil and

261 management input data perturbations. In the current analysis, we have sampled 500 joint

262 parameter / input data perturbation sets from the posterior distributions as reported by

263 Santabárbara, (2019) and we deployed them in simulations (propagation through the model)

264 for the regional inventory leading to 500 inventory simulations. A statistical analysis was,

265 afterwards, applied to estimate the updated regional and temporal result distributions.

266

267 2.5 Statistical methods and data aggregation

268 Regional result aggregation

269 One full regional inventory simulation consists of 10 individual inventory simulations: Five (5)

270 different crop rotations for irrigated and rain feed conditions were simulated in parallel (see

271 section 2.3). The results of the crop rotations were aggregated according to the crop shares

272 per year (see Table 2) accounting for all effects of the different crops cultivated in the region

273 for irrigated and rain feed conditions. The final inventory simulation results were obtained by

274 considering irrigated versus rain feed water management. The final inventory contains

275 simulation results aggregated to area weighted yearly means across the total simulation

276 domain accounting for the cropland area of each polygon.

277

278 Uncertainty quantification and statistical analysis

279 A regional aggregation was performed for all 500 uncertainty simulations. All the uncertainty

280 results were finally reported via statistical measures evaluating the 500 regional uncertainty

281 simulation runs reporting mean values, standard deviation, medians and the 25 and 75

282 interquartile ranges (IQR, Q25 to Q75).

283

284 3 Results Analysis and Evaluation

285 The simulation time span was from 2009 to 2016, while the years 2009 – 2011 were used as

286 spin-up to get all soil C and N pools into equilibrium after the initialization. Therefore, reported

287 simulation results are limited to years 2012 - 2016. The assessment of the regional C and N

288 balances (CB and NB) were obtained - as a consequence of the uncertainty quantification -

289 resulting in distributions and therefore reported by statistical measures such as mean/median

290 or interquartile ranges of the uncertainty ensemble.

291

292 3.1 Regional yield simulations and validation

293 The evaluation of the model performance in estimating the NB and CB components was

294 analyzed based on the comparison of the simulated yield values with the observed yield data

295 provided by the Hellenic Statistical Authority (ELSTAT), averaged for the total simulated

296 period.

297

298   Crop yields and feed production

299   For model validation, datasets of crop yields from Hellenic Statistical Authority (ELSTAT) were

300   used. Table 3 summarizes the aggregated regional crop yields for all the simulated years and

301   the respective mean, median and standard deviation values resulted from the statistical

302   analysis of the simulation results together with the observed yield and feed production provided

303   by the Hellenic Statistical Authority (ELSTAT). Simulated yields consist for cotton of the cotton

304   bolls, clover feed is the total cutting and harvested above ground biomass, for wheat and barley

305   is the grain yield and for maize is accounted grain ear and the stems. Based on the

306   observations, maize appears to be the dominant crop with an average yield of 12 tons ha^{-1},

307   followed by clover product of 8.4 tons ha^{-1}. The rest of the three crop yields appear to be in the

308   same order of magnitude from 3.3 up to 3.4 tons ha^{-1}.

309

310   *Table 3. Simulated and observed yields and feed production [tons dry matter ha^{-1}] in the region of Thessaly. All*
311   *results are based on statistical aggregation across all polygons, rotations, years and finally across all 500 UA*
312   *inventory simulations. The observed values of dry matter (DM) are provided by the Hellenic Statistical Authority.*

	Simulated crop yield and feed distributions [tons dry matter ha^{-1}]			Observed [tons dry matter ha^{-1}]
Crops	Median	Mean	standard deviation	Mean
Cotton	3.5	3.3	0.8	3.3
Clover	9.8	9.6	0.6	8.4
Wheat	3.9	3.6	0.9	3.4
Barley	4.7	4.5	1.0	3.3
Maize[1]	10.2	9.9	1.4	12.0

313   [1] *Observation data for maize did not distinguish between food corn and silage maize.*

314

315   Additionally, the simulated average yield of cotton was estimated to 3.3 ± 0.8 tons DM ha^{-1},

316   wheat to 3.6 ± 0.9 tons DM ha^{-1}, barley 4.5 ± 1 tons DM ha^{-1}, maize 9.9 ± 1.4 tons DM ha^{-1}. As

317   for the feed, the clover was estimated to 9.6 ± 0.6 tons DM ha^{-1}. The average nitrogen use

318   efficiency (NUE) across time and space is 63.29%.

319

320   Figure 1 presents the uncertainties of the simulated crop yield across the whole evaluation

321   time span 2012 -2016 both in irrigated and rain feed conditions. As shown, corn shows a much

322   more narrow distribution with a higher median for the irrigated scenario compared to the rain

323   feed while shows the same extreme value variations. To the contrary, winter barley has a wider

324   distribution and slightly higher median for the irrigated scenario and, also, a wider extreme

325   value variation. As for cotton, the distribution appears to be bimodal for the rain feed scenario

326   in which the median is also lower than the one in the irrigated case. In addition, the extreme

327   value variation is wider in the latter case. Finally, for the example of winter wheat irrigated and

328   rain feed scenarios reach the same results.

329
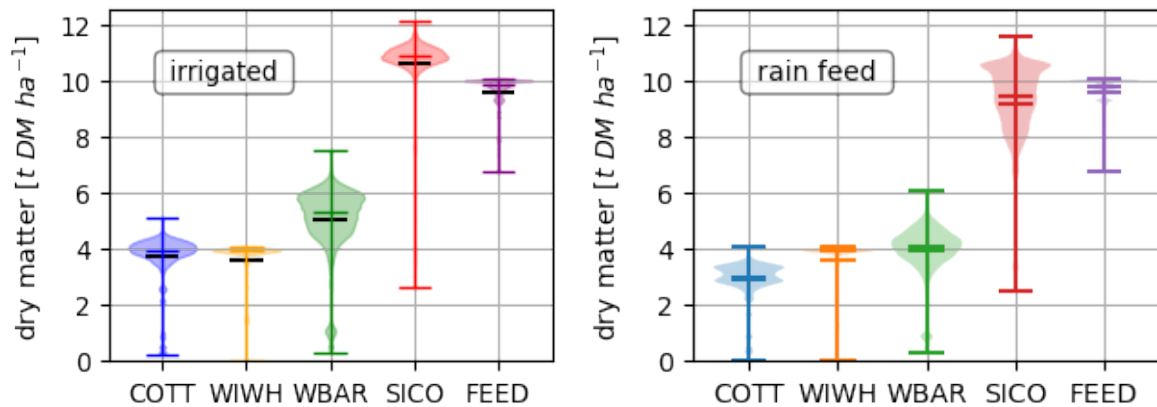
331   *Figure 1. Simulated crop yield uncertainties across the evaluation time span 2012 - 2016 for irrigated and rain feed*
332   *conditions. Horizontal lines indicate median, mean, maximum and minimum values of the distributions.*

333

334   3.2   Regional Carbon and Nitrogen Balance

335   Carbon Balance (CB)

336   For the CB, Figure 2 presents average C input fluxes into the soil of 12.4 ± 1.4 tons C ha^{-1} yr^{-}

337   ^{1} (with inter quartile ranges (IQR) from Q25 to Q75 of 12.1 to 13.2 tons C ha^{-1} yr^{-1}) and output

338   fluxes of 11.9 ± 1.3 tons C ha^{-1} yr^{-1} with IQR from 11.6 to 12.7 tons C ha^{-1} yr^{-1}. The resulting

339   carbon sequestration was estimated to 0.5 ± 0.3 tons C ha^{-1} yr^{-1} with IQR from 0.4 to 0.7 tons

340   C ha^{-1} yr^{-1} (data summarized in Table 4).

341
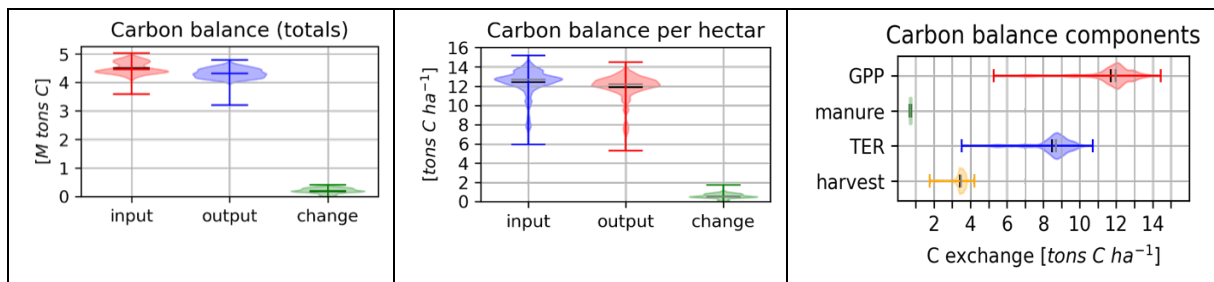
Figure 2. Carbon balance for cropland cultivation for the region of Thessaly: a) Total carbon balance of cropland soils in mio. tons C, b) averaged Carbon Balance in tons C ha^{-1} and c) averaged fluxes across the region and the years 2012-2016. (Positive change equals soil C sequestration).

345

The input fluxes consist of annual gross primary productivity (GPP) of 11.7 ± 1.4 tons C ha^{-1} yr^{-1} with IQR from 11.4 to 12.4 tons C ha^{-1} yr^{-1} and carbon applied to soils in manure estimated by 0.7 ± 0.001 tons C ha^{-1} yr^{-1} (see Table 4). This compares on the other hand to respirative carbon fluxes from the soil to the atmosphere (TER) of 8.5 ± 1.1 tons C ha^{-1} yr^{-1} with IQR from 8.2 to 9.1 tons C ha^{-1} yr^{-1} and carbon fluxes via exported crop yields and feed (including all straws and removed crop residues) of 3.4 ± 0.3 tons C ha^{-1} yr^{-1} with IQR from 3.4 to 3.6 tons C ha^{-1} yr^{-1}. The aggregation of the carbon fluxes to the regional level of approx. 360 000 ha of cropland results in 4.25 ± 0.20 M tons C yr^{-1} by GPP, 0.25 ± 0.01 M tons C yr^{-1} carbon influx via organic fertilizers compared to 3.08 ± 2.97 M t C yr^{-1} TER and 1.24 ± 0.05 M t C yr^{-1} carbon exports via crop yields and feed production leading to a net carbon sequestration of 0.5 ± 0.3 M tons C ha^{-1} yr^{-1} with IQR from 0.4 to 0.7 M tons C ha^{-1} yr^{-1} (M tons C as Million tons carbon).

357

*Table 4. **Carbon Balance** (per hectare) Assessment and Uncertainty Analysis of the of cropland cultivation at the region of Thessaly, Greece. [1] mean; [2] standard deviation; [3] median; Interquartile ranges: [4] Q25: 25 quartile, [5] Q75: 75 quartile are applied across the 500 values for the quantities in this table; [6] C-Inputs as the sum of the absolute values of all the input fluxes of the 500 simulations; [7] C-Outputs as the sum of the absolute values of all the output fluxes of the 500 simulations; [8] SOC-changes as the difference between the input and output fluxes of each of the 500 simulations. Note: The underlying arable management / crop rotations include the ploughing in of a perennial feed crop leading to large C inputs to the soil.*

	Mean[1]	Std[2]	Median[3]	Q25[4]	Q75[5]
	[tons C ha^{-1} yr^{-1}]	[tons C ha^{-1} yr^{-1}]	[tons C ha^{-1} yr^{-1}]	[tons C ha^{-1} yr^{-1}]	[tons C ha^{-1} yr^{-1}]

C-Inputs[6]	12.4	1.4	12.7	12.1	13.2
C-Outputs[7]	11.9	1.3	12.2	11.6	12.7
SOC-changes[8]	0.5	0.3	0.5	0.4	0.7
Input fluxes					
GPP	11.7	1.4	12.0	11.4	12.4
C in manure	0.7	0.0	0.7	0.7	0.7
Output fluxes					
TER	8.5	1.1	8.7	8.2	9.1
Biomass export	3.4	0.3	3.5	3.4	3.6

365

Nitrogen balance (NB)

367 In Figure 3 the assessment of the distribution of the NB with the in- and out-fluxes is presented.

368 The averaged nitrogen influx (represented by the uncertainty ensemble mean) per hectare was

369 estimated to 212.3 ± 9.1 kg N ha^{-1} yr^{-1} with IQR from 203.3 to 220.0 kg N ha^{-1} yr^{-1} while nitrogen

370 out-fluxes were estimated in average to 198.3 ± 11.2 kg N ha^{-1} yr^{-1} with IQR from 191.4 to

371 204.0 kg N ha^{-1} yr^{-1} (Figure 3) leading to a net N accumulation in the soil of 14.0 ± 2.1 kg N ha^{-1}

372 ^{1} yr^{-1} with IQR from 11.9 to 16.0 kg N ha^{-1} yr^{1}.

373
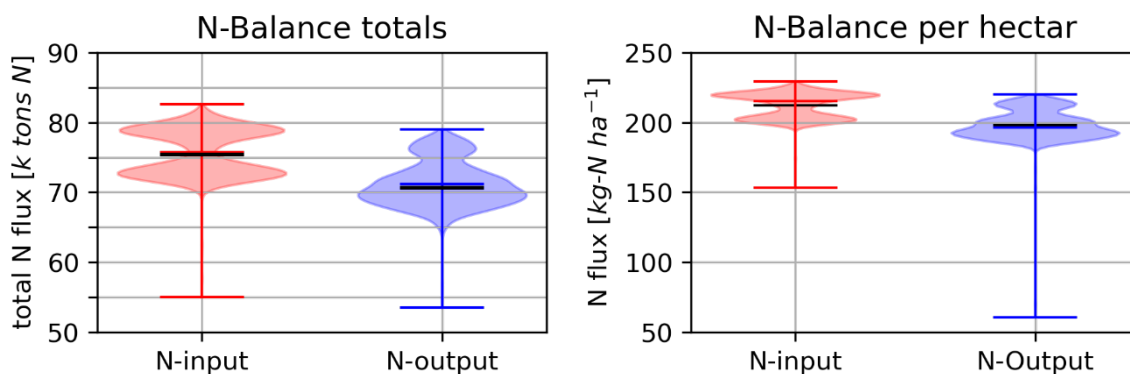
374

375 *Figure 3. Nitrogen balance for cropland cultivation for the region of Thessaly; a) Total NB in k-tons N and b)*
376 *averaged NB in kg N ha^{-1}; Data averaged for the years 2012-2016. Horizontal lines indicate mean (red), median*
377 *and minimum and maximum of the distribution.*

378

*Table 5. Nitrogen Balance (per hectar). Summary of the Assessment and Uncertainty Analysis of the **NB Fluxes** (per hectare) of cropland cultivation of the region of Thessaly, Greece. [1] N-Inputs as the sum of the absolute values of all input fluxes of the 500 simulations; [2] N-Outputs as the sum of the absolute values of all the output fluxes of the 500 simulations; [3] N-stock-changes as the difference between the input and output fluxes of each of the 500 simulations; [4] Gaseous emissions are the sum of N_2O, NO, N_2 and NH_3 fluxes; [5] Aquatic flux is nitrate leaching (NO_3^-).*

	Mean	Std	Median	Q25	Q75
	[kg N ha^{-1} yr^{-1}]	[kg N ha^{-1} yr^{-1}]	[kg N ha^{-1} yr^{-1}]	[kg N ha^{-1} yr^{-1}]	[kg N ha^{-1} yr^{-1}]
N-Inputs[1]	212.3	9.1	215.2	203.3	220.0
N-Outputs[2]	198.3	11.2	196.4	191.4	204.0
N-stock-changes[3]	13.8	2.1	13.7	14.5	12.5
Input fluxes					
N deposition	6.3	0.8	6.8	6.0	6.8
Bio. N fixation	45.6	4.3	45.7	43.7	47.7
N in min. fertilizer	80.2	4.8	81.3	76.6	82.7
N in organic fertilizer	80.2	3.6	80.9	77.5	82.7
Output fluxes					
Gaseous emissions[4]	55.4	8.8	55.1	48.9	61.6
N_2O	2.6	0.8	2.5	2.1	3.1
NO	3.2	1.5	2.9	2.0	4.1
N_2	15.5	7.0	14.6	9.9	20.7
NH_3	34.0	6.7	31.8	29.3	36.9
Aquatic fluxes[5]					
NO_3 leaching	14.1	4.5	13.6	11.0	17.0

The N influx was composed by the input of synthetic fertilizer of 80.2 $\pm$ 4.8 kg N ha^{-1} yr^{-1} (IQR 76.6 to 82.7) and organic fertilizer of 80.2 $\pm$ 3.6 kg N ha^{-1} yr^{-1} (IQR from 77.5 to 82.7), followed by the biological nitrogen fixation (BNF) via legumes estimated as 45.6 $\pm$ 4.3kg N ha^{-1} yr^{-1} (IQR from 43.7 to 47.7) and nitrogen deposition of 6.3 $\pm$ 0.8kg N ha^{-1} yr^{-1} (IQR from 6.0 to 6.8). Thus, almost 75% of the nitrogen input influx is related to the fertilization (mineral and organic) whilst the minor part that corresponds to nitrogen fixation and deposition approximates to 25%.

392   The N outflux consist of gaseous N fluxes of 55.4 ± 8.8 kg N ha⁻¹ yr⁻¹ (IQR from 48.9 to 61.6),

393   aquatic N fluxes (only nitrate leaching into surface waters was considered) of 14.1 ± 4.5 kg N

394   ha⁻¹ yr⁻¹ (IQR from 11.0 to 17.0), N fluxes by removed N in yields, straw and feed of 128.8 ±

395   8.5 kg N ha⁻¹ yr⁻¹ (IQR of 125.2 to 131.7) (see Figure 4 and Table 5). Based on the

396   aforementioned results all gaseous and aquatic N-fluxes correspond to about 28% and 7% of

397   the N output flux respectively, while the far largest N output flux was N removed in yields, straw

398   and feed representing almost 65% of the N outflux (Figure 4).
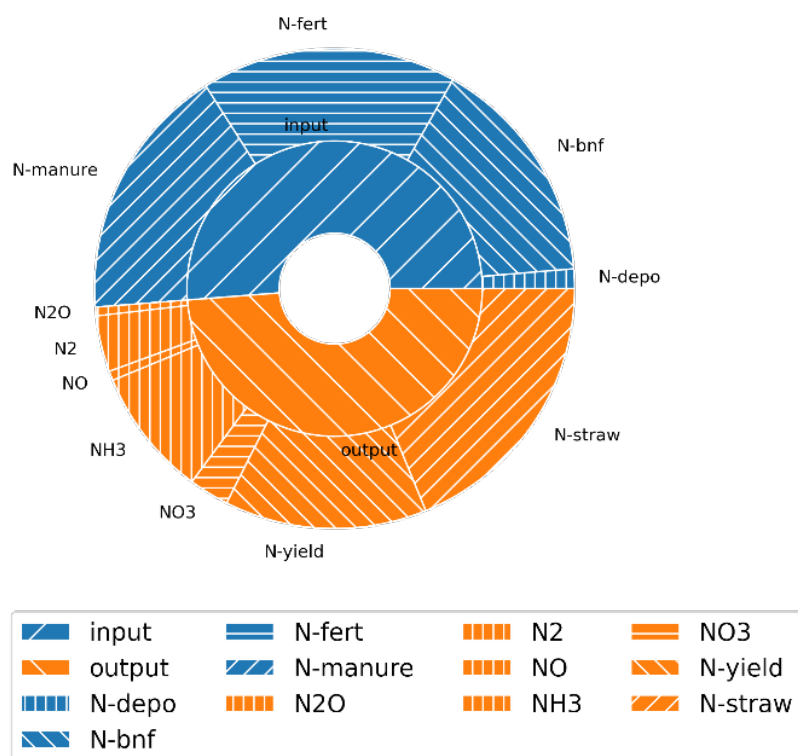
399

400   *Figure 4. Averaged annual nitrogen balance (inner ring of the pie diagram) and their decomposition into the various*
401   *components of the N fluxes (outer ring of the pie diagram); (all data summarized in Table 5).*

402

403   The simulated gaseous fluxes were composed of N_2O emissions estimated to 2.6 ± 0.8 kg

404   N_2O-N ha⁻¹ yr⁻¹ (IQR from 2.1 to 3.1), NO emissions of 3.2 ± 1.5 kg NO-N ha⁻¹ yr⁻¹ (IQR from

405   2.0 to 4.1), N_2 emissions 15.5 ± 7.0 kg N_2-N ha⁻¹ yr⁻¹ (IQR range from 9.9 to 20.7) and NH_3

406   emissions of 34.0 ± 6.7 kg NH_3-N ha⁻¹ yr⁻¹ (IQR from 29.3 to 36.9). Ammonia volatilization

407   represents the largest share (61.48%) of gaseous N losses, with highest densities in the

408   emission distribution between approx. 25 and 35 kg N ha⁻¹, followed by di-nitrogen losses

409   (28.03%) of gaseous N losses, with a much wider emission variability in the distribution,

410   followed by NO_3 (5.79%) and N_2O (4.7%). Figure 5 shows the overall NB in a waterfall diagram

411   adding up cumulative all in- and out-fluxes illustrating the uncertainty distribution of each flux

412   contributions. The waterfall diagram illustrates the overall outcome of the NB, a N accumulation

413   into the soil as the difference between all out-fluxes minus all in-fluxes.

414
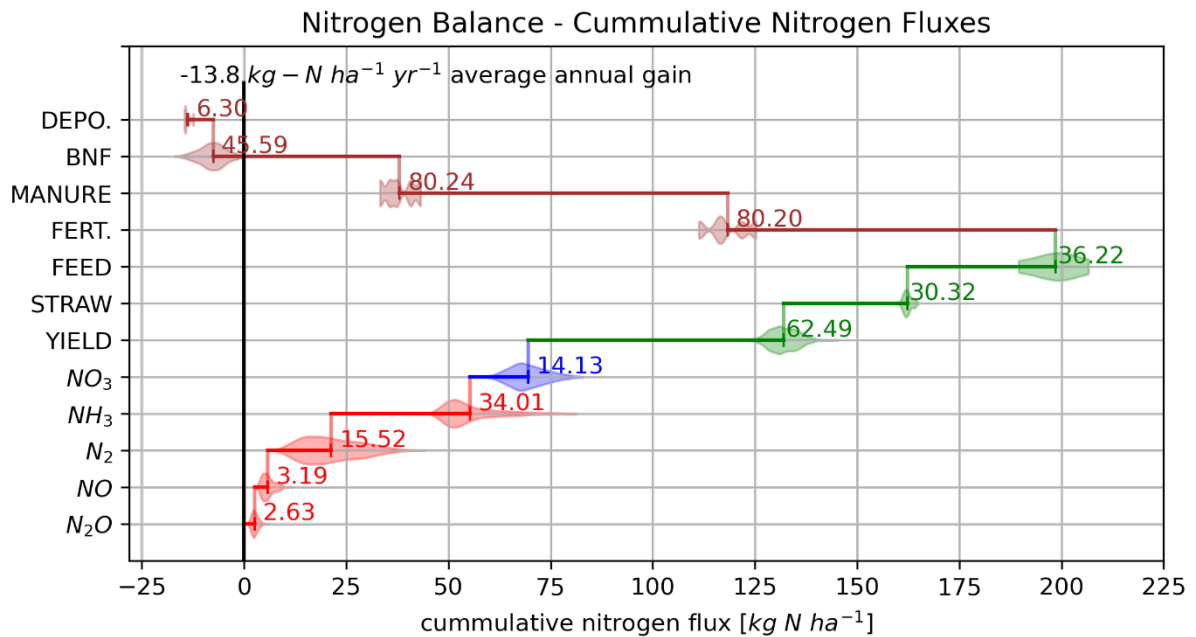
415

416 *Figure 5. Waterfall representation of the result distributions of the different Nitrogen in- and outfluxes of the cropland*
417 *cultivation in Thessaly. Vertical lines in the distributions indicate mean values of the corresponding N-flux. Red*
418 *colors indicate gaseous outfluxes, blue aquatic fluxes, green biomass yield and feed production outfluxes and brown*
419 *color indicates N influxes such as synth. N-fertilizer, N-Manure, biological N fixation (BNF) and N deposition. The*
420 *Resulting N sink of the Nitrogen Balance (based on distribution means) is -13.8 kg N ha^{-1} yr^{-1}. (Negative value*
421 *indicates flux into the soil).*

422

423   Nitrate leaching mean estimates were 14.1 ± 4.5 kg NO_3-N ha^{-1} yr^{-1} (IQR from 11.0 to 17.0)

424   with a bell-shaped distribution.

425   Total yield and biomass (straw and feed) N export fluxes were 62.4 ± 4.4 kg N ha^{-1} yr^{-1} with

426   uncertainty ranges from 59.9 to 65.1 consisting of yield N exports (grains and cotton balls) of

427   30.3 ± 1.7 kg N ha^{-1} yr^{-1} (IQR from 29.6 to 30.9) and for straw and feed N exports of 36.1 ± 6.0

428   kg N ha^{-1} yr^{-1} (IQR from 34.9 to 37.6). The result distributions for yield N are well bell shaped,

429   for feed biomass N very moderate bell shaped and well distributed within the bounds and for

430   straw N very sharp within a comparable small interval.

431   Figure 5 illustrates the cumulative nitrogen fluxes composing the NB as a waterfall diagram

432   considering the mean of each component. The NB results in a net N sink of 13.8 kg N ha^{-1} yr^{-}

433   ^{1} (see result distribution in Figure 6) for the region corresponding to an annual carbon

434   sequestration of approx. 0.5 tons C ha^{-1} yr^{-1} as depicted in Figure 2 b) (see also the annual

435   dynamics of the topsoil (30 cm) soil organic carbon and nitrogen distributions in Figure 8).

436
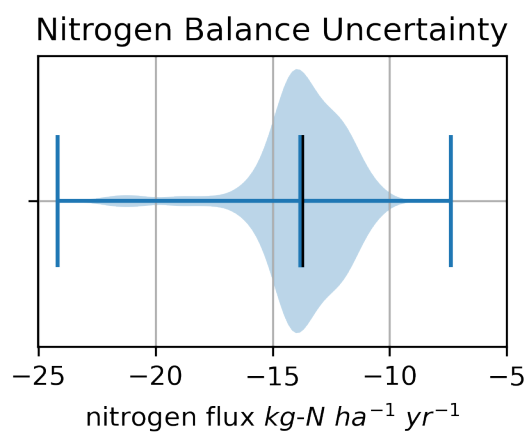
437

438   *Figure 6. Distribution of the overall Nitrogen Balance of the cropland cultivation in Thessaly: Statistical analysis*
439   *across all 500 individual NB results of the inventory simulations (mean 13.8 kg N ha^{-1} yr^{1}, median 13.7 kg N ha^{-1}*
440   *yr^{1}) corresponding to the Carbon balance in Figure 2.*

441

442   Figure 7 and Figure 8 show the dynamics of the annual distribution of the gaseous and aquatic

443   outfluxes as well as the dynamics of the annual distributions of the top soil (30 cm) soil organic

444   carbon and nitrogen pools for the evaluation period 2011 – 2016.
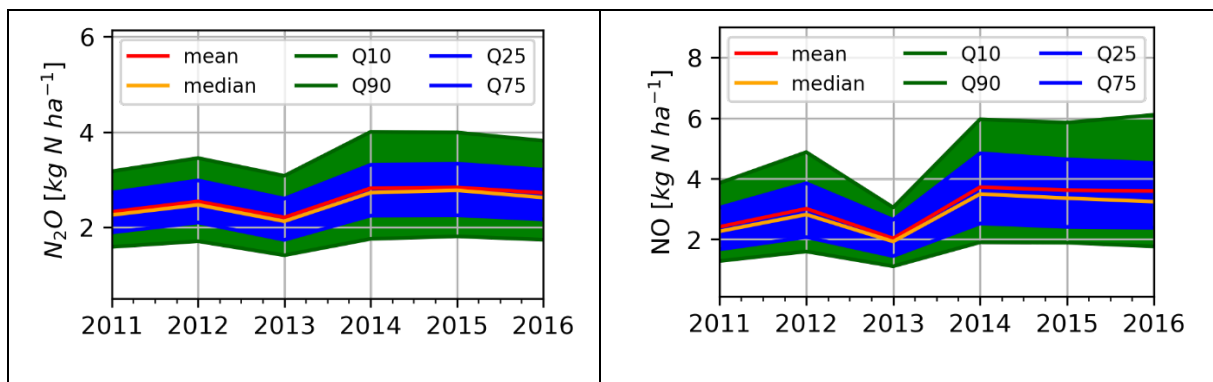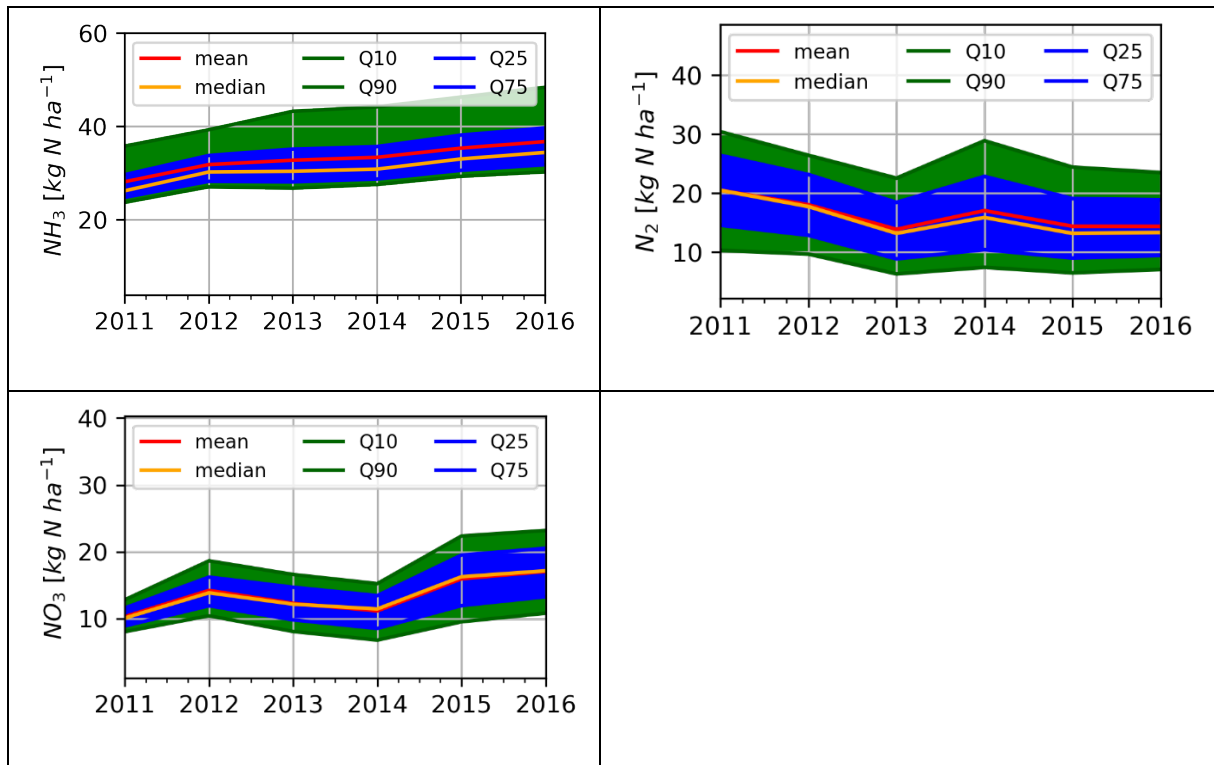
445 *Figure 7. Annual dynamics of the uncertainty distributions of the gaseous (subfigure a) to d)) and aquatic (subfigure*
446 *e)) N outfluxes 2011 – 2016. Uncertainty bandwidth (blue band) defined as the range between the q25 and the q75*
447 *quartile, green band (Q10. to Q90 interval) indicating the variance of the fluxes neglecting the outliners of the*
448 *distribution.*

449

4   Discussion.

In this study, following the recommendation of Grosz et al., (2023), an assessment of the combined full C and N balance of a regional cropland agroecosystem is reported for the first time using inventory simulations with a process-based ecosystem model. The additional quantification of the associated modelling uncertainty of the balance simulations increase the trustworthiness of the study.

Up to present, process-based modelling studies mainly focus on single site applications e.g. Daycent: (del Grosso et al., 2005; Gurung et al., 2020), APSIM: (Vogeler et al., 2013), CERES-EGC: (Dambreville et al., 2008; Gabrielle et al., 2006; Heinen, 2006; Hénault et al., 2005), CERES-Wheat: (Mavromatis, 2016), DNDC: (Li, 2000), LandscapeDNDC: (Haas et al., 2013; Klatt et al., 2015a; Molina-Herrera et al., 2016; Zhang et al., 2015). Fewer studies deploy models on the regional to national (del Grosso et al., 2005; Kim et al., 2015; Klatt et al., 2015a) or continental to global scale (del Grosso et al., 2009; Franke et al., 2020; Jägermeyr et al., 2021; Smerald et al., 2022; Thompson et al., 2019). All of these studies are subject to criticism stated by Grosz et al., (2023) as they are reporting in general only one specific or a few components of the carbon or nitrogen cycle such as e.g. soil carbon stocks or N_2O emissions, lacking any information on the full C and N balance.

There are only a very few cases where an attempt for regional estimation of the NB has been made. The study reported by Schroeck et al., (2019) is the only previous attempt fulfilling the requirements of Grosz et al., (2023) in reporting the full NB for a large alpine watershed in the Austrian Alps characterized by arable production in the low-lying areas and grassland in the mountains using a process based model. In addition, Lee et al., (2020) tried to estimate nitrogen balances in Switzerland alternating the cropping systems or management practices. There were, also, cases where the regional NB was estimated with the use of nitrogen balance equations (He et al., 2018). Recently, Zistl-Schlingmann et al., (2020) assessed the full N balance of alpine grasslands using the ^{15}N stable isotope techniques.

479   In order to achieve a more concrete and complete analysis of the CB and NB that could be

480   used for future policy development, an uncertainty analysis is considered as

481   necessary/mandatory. The IPCC guidelines demand for UNFCC reporting the uncertainty

482   quantification of any reported inventory study (IPCC Updated guidelines 2019). Recent

483   publications have reported the deployment of different methods to assess and quantify the

484   various sources of uncertainty in ecosystem modelling. (Klatt et al., 2015b) published a study

485   on the impact of parameter uncertainty on N_2O emissions and NO_3 leaching on the regional

486   scale. (Houska et al., 2017) deployed the GLUE method (Generalized Likelihood Uncertainty

487   Estimation) for the LandscapeDNDC model on a grassland site, other studies such as

488   (Lehuger et al., 2009a; Li et al., 2015; Myrgiotis et al., 2018a) used the Bayesian Model

489   Calibration and Uncertainty Assessment approach, which has been used in the current study

490   as well.

491

492   4.1   Yield and feed Production

493   LandscapeDNDC was validated in a study by Molina-Herrera et al., (2016) on cropland and

494   grassland sites across Europe reporting good agreement in reproducing observed above

495   ground biomass and yield estimates. Similar model performance for the cultivation of

496   commodity crops was reported by (Kasper et al., 2019; Klatt et al., 2015a; Molina-Herrera et

497   al., 2017; R. J. Petersen et al., 2021).

498   Lyra and Loukas, (2021) used REPIC model to estimate the crop growth/yield production of

499   several crops in the Basin of Almyros, Thessaly. The simulated results were approximately 11

500   tons ha^{-1} clover, 3.3/3.5 tons ha^{-1} cereals/wheat, 3.8 tons ha^{-1} cotton and 9 tons ha^{-1} maize,

501   being well compared to the results of our research shown in Table 3. The simulated results

502   presented in our study are in line with the results by Voloudakis et al., (2015) simulating cotton

503   production in seven different areas of Greece applying the AquaCrop model. Similar results

504   were reported by (Tsakmakis et al., 2019).

There are few cases in literature concerning yield simulations on a European level. Based on the yield datasets of FAO and EUROSTAT, Ciais et al., (2010a) estimated mean crop yields for the period 1990–1999 at the scale of EU-25 as 6.1 (FAO) and 5.3 (EUROSTAT) tons DM ha^{-1} yr^{-1}, respectively, which corresponds well to results of our study. Haas et al., (2022) estimated with a model ensemble mean for crop yields for EU-27 of 4.41 ± 1.85 tons DM ha^{-1} yr^{-1} for the period 1990–1999. Lugato et al., (2018) estimated cropland yield projections of 4.34 tons DM ha^{-1} yr^{-1} (mean), ranging from 3.69 to 4.90 tons DM ha^{-1} yr^{-1} with the DayCent model for EU-27, comparable to the 6.18 tons DM ha^{-1} yr^{-1} average simulated crop yields of this study. The simulated yields in the current study vary from 3.3 to 9.9 tons DM ha^{-1} yr^{-1} for the cases of cotton and maize respectively.

Higher yield estimates for the region of Thessaly in this study are certainly due to the inclusion of the legume feed crops in the rotations. This argument is supported by a recent meta-analysis by (Lu, 2020) that concluded that on average yield increases of 5.0 to 25% can be expected for various conditions if residues are completely returned to the field as compared to no-residue return systems. Similar results were reported by Fuchs et al., (2020) and Barneze et al., (2020). Following the recommendations of Grosz et al., (2023), our study has reported transparently all major C & N fluxes for the region as being simulated by the model. In our study, we have not calibrated the model against any observations, therefore all simulation results will be discussed versus other modelling results available. As up to now, there is only one comparable modelling study available in literature reporting and discussing the total N balance of a site or region, which we have used to compare our N balance against.

4.2 Carbon and Nitrogen Balance:

Full N balance

At present, the studies of Schroeck et al., (2019) and Lee et al., (2020) are the only to be found by Web of Science under the search key words "nitrogen AND balance AND process AND based AND modelling" reporting a compilation of the nitrogen balance and all associated N

532   fluxes for a site or region applying a process-based ecosystem model as demanded by Gosz

533   et al (2023).

534   Leip et al., (2011) reported the first nitrogen balance for Europe following a mixed approach

535   combining the CAPRI (Common Agricultural Policy Regionalised Impact) model (a global

536   economic model for agriculture) with different approaches estimating various nitrogen fluxes

537   in arable land cultivation, but the approach lacks the explicit quantification of the different

538   gaseous N fluxes. The study of Schroeck et al., (2019) overcame this hurdle and applied the

539   process-based ecosystem model LandscapeDNDC to estimate the full regional nitrogen

540   budgets including all fluxes of different ecosystems (cropland, grassland and pastures) and

541   climatic zones of a water shed in Austria. That has been the first attempt estimating and

542   reporting all the N fluxes possible as demanded by Gosz et al (2023).

543   The N balance estimate in Schroeck et al., (2019) for a catchment in Austria and the N balance

544   reported in our study compares very well despite the inherent differences in land management

545   and N inputs. As highlighted by Grosz et al., (2023), such intercomparisons demonstrate the

546   different model behaviours when applied to different ecosystem. In our study, we see the

547   partitioning of the N outfluxes from our arable system in similar shares as reported by Schroeck

548   et al., (2019) for the arable land.

549   The N_2O estimate in Schroeck et al., (2019) and the current study is of a comparable level. We

550   estimated N_2O emissions of 2.6 kg N ha^{-1} yr^{-1} while Schroeck et al., (2019) reports 1.51 kg N

551   ha^{-1} yr^{-1}, about 40% lower. The NO fluxes differ significantly since we reported a mean value

552   of 3.2 kg NO-N ha^{-1} yr^{-1} while Schroeck et al., (2019) reports 0.08 kg NO-N ha^{-1} yr^{-1}. This is

553   on one hand related to some recent model advances, which have been made during this study,

554   which elevated the NO production in LandscapeDNDC (Molina-Herrera et al., 2017) and on

555   the other hand due to the high share of organic N fertilization in our study fostering NO

556   emissions. Ammonia volatilization differs substantially between the two studies, while our study

557   reports 34 kg NH_3-N ha^{-1} yr^{-1}, Schroeck et al., (2019) reported moderate emissions of 0.23 kg

558   NH_3-N ha^{-1} yr^{-1}. The strong NH_3 volatilization in our study is mostly driven by the high pH-

559   values of the soils in the region of Thessaly (pH values from 6.5 to 8.2 with a considerable

spatial variation, Greek Soil Map, 2015) and the comparable high manure inputs into the arable system in our study, while in the research of Schroeck et al., (2019) the manure was preferably applied only to the grassland systems and mineral fertilizers to the arable land. Concerning the NO_3, Schroeck et al., (2019) reported 45.3 kg NO_3-N ha^{-1} yr^{-1} which was 3 times higher compared to this study (14.1 kg N ha^{-1} yr^{-1}) considering the N-input of approximately 160 kg and 212.3 kg N ha^{-1} yr^{-1} respectively. Even though 50 % or the arable land in our study was irrigated, the resulting water percolation rates in our study were by far lower than the percolation simulated in the study of Schroeck et al., (2019) as the Austrian pre-alpine catchment received nearly double annual precipitation.

The N balance modelling study of Lee et al., (2020) was estimating for Switzerland a national cropland N balance using an upscaling method based on process-based site simulations with the DayCent model differentiating the management of the considered cropping systems e.g. fertilizer rates, tillage or land cover change. The study reported for conventional cultivations (averaged across 20 years) yield related N outfluxes accounting for about 60%, NO_3 leaching 36.1% and gaseous N emissions 4.1% of the total N outputs. Lee et al., (2020) did not report the different gaseous N fluxes, even though the DayCent model must have simulated all of them. Although the yield related N outflux is in accordance with our result of 64.95% there seems to be a discrepancy in the reported gaseous and aquatic N fluxes contribution, as we report 27.94% for gaseous and 7.11% for NO_3 leaching in our study. As demanded by Gosz et al (2023) we can elaborate different preferences in simulated N outflux partitioning (36% NO_3 and 4% gaseous losses for DayCent versus 7% NO_3 and 28% gaseous losses for LandscapeDNDC) due to the different simulation models, regionalization and upscaling approaches as well as due to the different soil, climatic and management conditions included in the respective studies.

Velthof et al., (2009) used the MITTERA-EUROPE model/method, based on the concoction of GAINS and CAPRI models, to estimate N fluxes of European soils on NUTS2 scale with the use of European datasets and literature coefficients, where the fertilizer application and management was similar to our methodology. The average N Input-Output balance was

588   calculated as 117 kg N ha^{-1} yr^{-1} composed by manure of 49 kg N ha^{-1} yr^{-1}, synthetic fertilizer of

589   58 kg N ha^{-1} yr^{-1} (in the current study for both cases 80.2 kg N ha^{-1} yr^{-1}), biological nitrogen

590   fixation of 2 kg N ha^{-1} yr^{-1} (our research 45.6 kg N ha^{-1} yr^{-1}) and N deposition of 7 kg N ha^{-1}

591   (current study 6.3 kg N ha^{-1} yr^{-1}). In contrast to our study the reported output fluxes for NH_3 of

592   8 kg NH_3-N ha^{-1} yr^{-1}, N_2O of 2 kg N_2O-N ha^{-1} yr^{-1}, NO_x of 2 kg NO_x-N ha^{-1} yr^{-1}, N_2 of 51 kg N_2-N

593   ha^{-1} yr^{-1} and NO_3 leaching of 7 kg NO_3-N ha^{-1} yr^{-1} while the differences with the results presented

594   in our study are NH_3 of 34.0 kg NH_3-N ha^{-1} yr^{-1}, N_2O of 2.6 kg N_2O-N ha^{-1} yr^{-1}, NO_x of 3.2 kg

595   NO_x-N ha^{-1} yr^{-1}, N_2 of 15.5 kg N_2-N ha^{-1} yr^{-1} and NO_3 leaching of 14.1 kg NO_3-N ha^{-1} yr^{-1}.

596   Additionally, the yield output is estimated as 48 kg N ha^{-1} yr^{-1}. Again, we see a different

597   preference in N outflux partitioning towards large shares in gaseous N fluxes versus small NO_3

598   leaching shares and the difference with the results presented in our study are related to the

599   different input data used for initialization and driving of the model, based on regional statistics

600   and the use of a biogeochemical model versus emission factor approaches.

601   He et al., (2018) assessed the soil N balance for a time spam between 1984 to 2014 based on

602   the N budget equations (N input – N output) using multiple coefficients from literature in order

603   to estimate the nitrogen input and output fluxes of six grouped regions in China. The used

604   datasets were acquired from national Authorities and include cropping land and yields,

605   synthetic fertilizers, animal heads, soil types etc. The N synthetic fertilizer input is in average

606   182.4 kg N ha^{-1} and the organic fertilizer of 97.3 kg N ha^{-1}, N fixation is estimated as 16.8 kg

607   N ha^{-1} and the atmospheric deposition as 22 kg N ha^{-1}. Almost half of the total averaged N

608   output losses, 48.9%, was attributed to crop uptake while the respective gaseous losses were

609   N_2 19.9%, volatilized NH_3 17.3%, N_2O 1.2% and NO 0.7%. As for the NO_3 leaching share was

610   5.8% of the total output N fluxes. These reported N outflux proportions comparable well to our

611   study. The differences in the N uptake data remain and are mainly due to the differences in

612   the crops and management.

613   As reported in OECD (OECD, 2020) the net averaged nitrogen balance of the area of our study

614   is 11.6 kg N ha^{-1} yr^{-1} input to the soil which corresponds very well to the simulated mean

615   nitrogen balance as an in-flux of 13.8 kg N ha^{-1} yr^{-1} (IQR 11.9 to 16.0) into the soil.

616 So far, the discussion of the presented N balance and N out fluxes compares well to most of

617 the available studies reporting N balances while one modelling study report different N outflux

618 partitioning between gaseous and NO_3 leaching fluxes. For more detailed intercomparison on

619 the overall quality of our C and N fluxes we aim to compare our results versus various studies

620 addressing individual components of the C and N balance and associated fluxes.

621 SOC stocks

622 Haas et al., (2022) reported results of a European inventory simulation of soil carbon stocks

623 and N_2O emissions using a model ensemble. The study deployed in a baseline simulation

624 across EU-27 a similar residues management as compared to our study resulting in very stable

625 carbon stock dynamics over a long period (1950-2100). In this study, the estimated carbon

626 sequestration of 0.5 (UA mean and median) $\pm$ 0.3 tons C ha^{-1} yr^{-1} is mainly caused by the

627 inclusion of legume feed crops within the crop rotation leading to increased litter production

628 and C input into the soil (Barneze et al., 2020; Fuchs et al., 2020; K. Petersen et al., 2021).

629 Haas et al., (2022) reported a management scenario with 100% of crop litter remaining on the

630 field leading to averaged C-sequestration rates of over 1 ton C ha^{-1} yr^{-1} across EU-27. As the

631 residues management in this study is between the baseline and buried scenario of Haas et al.,

632 (2022), our results compare well to results reported in this study.

633 Other modelling studies such as (Lugato et al., 2014) reported C sequestration rates for the

634 conversion of cropland into grassland ranging between 0.4 and 0.8 tons C ha^{-1} yr^{-1}. Lugato et

635 al., (2014) reported averaged SOC change rates for a cereal straw incorporation scenario for

636 EU-27 of 0.1 tons C ha^{-1} yr^{-1} (estimates from 2000 to 2020).

637 The SOC dynamics reported in this study show a stable carbon dynamic in the soil within the

638 simulation time span (2009 - 2014) with only three years of model spin-up. The initialization of

639 the various carbon pools with the SOC data from the soil database is balanced by the average

640 litter production of the deployed crop rotations. The SOC increase in 2015 and 2016 is due to

641 climatic conditions and higher litter inputs simulated by the model.

642

643   N$_2$O emissions

644   This study reported estimates of N$_2$O emissions of 2.6 ± 0.8 kg N$_2$O-N ha^{-1} yr^{-1} (IQR from 2.1

645   to 3.1) for a mixed crop / legume feed crop rotation, which were well above the estimates

646   resulting from IPCC Tier I direct emission factors, IPCC would lead to 1.6 kg N$_2$O-N ha^{-1} yr^{-1}

647   when applying 30pprox.. 160 kg N ha^{-1} yr^{-1}. The higher N$_2$O emission strength of the modelling

648   is likely to result from emission peaks after irrigation due to low anaerobicity (Grosz et al.,

649   2023; Janz et al., 2022). Cayuela et al., (2017) conducted a meta-analysis of the direct N$_2$O

650   emissions for a number of cropping systems for the Mediterranean climate where the emission

651   factors (Efs) were altered under different fertilization and irrigation conditions. Higher

652   fertilization rates led to higher Efs (0.82% less than the 1% of IPCC). Additionally, irrigated and

653   intensively cultivated crops had higher Efs than rainfed (up to 0.91% dependent on the

654   irrigation method). The relatively high EF of maize in this study could be possibly attributed to

655   the irrigation without the application of water-saving methods and the on average higher N

656   application rates .

657   The LandscapeDNDC validation study of Molina-Herrera et al., (2016) reported for the Italian

658   site Borgo Cioffi (Mediterranean climate, Ranucci et al., (2011) annual N$_2$O emissions of 2.49

659   kg N$_2$O-N ha^{-1} yr^{-1} while two sites in southern France showed annual N$_2$O emissions from 0.52

660   to 3.34 kg N$_2$O-N ha^{-1} yr^{-1}. N$_2$O emission estimates of our study were higher than results

661   reported by Haas et al., (2022) using a multi model ensemble estimating average soil N$_2$O

662   emissions from European (EU-27) cropping systems for the period 1980–1999 of 1.46 ± 1.30

663   kg N$_2$O-N ha^{-1} yr^{-1} under conventional (*Baseline*) management and comparable average N

664   input. Klatt et al., (2015a) reported for an inventory (Saxony, Germany) mean N$_2$O emission

665   of 1.43 ± 1.25 kg N$_2$O-N ha^{-1} yr^{-1}..

666   Overall, the reported N$_2$O flux component of our study compares well to the findings

667   reported in literature. As critizised by Grosz et al. (2023), many studies only focus on the

668   performance of the models in simulating N$_2$O emissions and the models were even

669   calibrated for this purpose. Without reporting all the other N fluxes from the models, this

670 focusing and calibration for only one quantity can easily lead to inaccuracies for other

671 components of the N cycle as they may not be checked for consistency anymore.

672 Janz et al., (2022)Janz et al., (2022)

673 Nitrate leaching

674 This study reported average NO_3 leaching fluxes (only nitrate leaching into surface waters) of

675 14.1 ± 4.5 kg NO_3-N ha^{-1} yr^{-1}. Reported nitrate leaching observations for the region or Greece

676 could not be found in literatureestimated the NO_3 leaching with the use of four different models

677 with varying values from 5 to 40 kg NO_3-N ha^{-1} yr^{-1} for the area of our study. These high values

678 could be explained by the fact that it corresponds both to groundwater and runoff. Molina-

679 Herrera et al., (2016) reported for the LandscapeDNDC validation study cropland nitrate

680 leaching fluxes of approx. 7 to 88 kg NO_3-N ha^{-1} yr^{-1}. In addition, in the research of Molina-

681 Herrera et al., (2017) the described NO_3 leaching results varied from 13 to 8 kg NO_3-N ha^{-1} yr^{-1}

682 ^{1} showing higher values in regards to the precipitation and fertigation. The most comparable

683 site Borgo Cioffi resulted in a comparable annual NO_3 leaching flux of 18.62 kg NO_3-N ha^{-1} yr^{-1}

684 ^{1}.

685 Klatt et al., (2015b) reported in an uncertainty assessment for a regional inventory (Saxony,

686 Germany) leaching rates of 29.32 ± 9.97 kg NO_3-N ha^{-1} yr^{-1} for a wheat-barley-rapeseed

687 rotation simulated by the LandscapeDNDC model. The agricultural system and management

688 regime is comparable; higher NO_3 leaching rates were most likely due to high N fertilization

689 rates in combination with higher annual precipitation in the region leading to more intense

690 percolation and therefore to stronger leaching of available NO_3 while in our study the

691 fertilization regime was more lean such that soil nutrient competition was higher and available

692 nitrate was more likely to be immobilized by plant uptake. Myrgiotis et al., (2019) reported in a

693 similar assessment NO_3 leaching factor (LF) mean for their region of 14% (±7 %), in

694 comparison we report mean NO_3 leaching factor of 7%.

695

696 NO emissions

697 In the current study, the model estimated NO emissions were in average 3.2 ± 1.5 kg NO-N

698 ha^{-1} yr^{-1}. Butterbach-Bahl et al., (2009) performed the very first European inventory of soil NO

699 emissions using a modified version of DNDC reporting low NO emission rates mostly below 2

700 kg NO-N ha^{-1} yr^{-1}. Molina-Herrera et al., (2017) recently reported a full NO emission inventory

701 for the State of Saxony Germany compiling annual NO emissions from agricultural soils

702 ranging from 0.19 to 6.7 kg NO-N ha^{-1} yr^{-1} simulated by LandscapeDNDC. The study reported

703 the model performance on simulating soil NO emissions on more than 20 different sites. The

704 study of Schroeck et al., (2019) reported for a regional inventory of arable soils in Austria

705 simulated by LandscapeDNDC annual NO emissions of 1.0–1.5 kg NO-N ha^{-1} (for the year

706 2000), while empirical approaches such as Stehfest and Bouwman, (2006) estimated emission

707 of similar magnitude. Zhang et al., (2015) reported in a model inter-comparison and validation

708 study of NO and N_2O fluxes including three ecosystem models, consistent simulation results

709 for the LandscapeDNDC model with NO emission strengths of cropland soils were between 1

710 and 3 kg NO-N ha^{-1} yr^{-1} across the sites.

711

712 NH$_3$ emissions

713 Schroeck et al., (2019) stated that validation studies of NH$_3$ volatilization for any

714 biogeochemical model were very rarely reported in literature, mainly due to the complexity and

715 a lack of flux observations at spatial and temporal high resolution.

716 In our study we estimate soil NH$_3$ emissions of 34.0 ± 6.7 kg NH$_3$-N ha^{-1} yr^{-1}. High NH$_3$

717 volatilization and emission rates can be explained by the predominating neutral to basal soils

718 conditions (pH values of 7 and above) in the study region favouring the Henry NH$_4$/NH$_3$

719 equilibrium towards higher NH$_3$ gases enabling ammonia to diffuse out of the soil into the free

720 atmosphere.

721   The IPCC emission factor (EF) method for NH_3 volatilization reports estimates of 20% of N

722   input into the soil to be volatilized as NH_3. For our study, IPCC methodology for NH_3 would

723   lead to 32 kg NH_3-N ha^{-1} yr^{-1}, which is well in line with the simulated result.

724   Sidiropoulos and Tsilingiridis, (2009) estimated a national livestock originated NH_3 emission

725   corresponding to approx. 22 kg ha^{-1} yr^{-1} for the region of Thessaly.

726   There is a number of national NH_3 inventories which could be considered detailed and well-

727   studied like the ones in Denmark, Netherlands, Europe, UK and US. In Denmark, (Geels et al.,

728   2012) used the DAMOS model to estimate the Danish NH_3 emissions (crop, grass and manure

729   manipulation) where the values ranged in the 5 regions under study from a very small quantity

730   to 17.4 kg NH_3-N ha^{-1} yr^{-1}.

731   As discussed by Sutton et al., (2013) the majority of the NH_3 emissions come as a result of the

732   agricultural production and are considerably impacted by climate influence. In the case of NH_3

733   volatilization, it could almost double every 5°C temperature given certain complex

734   thermodynamics dissociation and solubility, whilst soil NH_3 emission is influenced by the

735   available water quantity allowing the NH_x dissolution and use by microbial organisms, which is

736   afterwards leading to decomposition.

737

738

739   4.3   Uncertainty Analysis and Quantification

740   Santabárbara, (2019) used the MCMC algorithm to estimate the joint parameter distribution of

741   the fundamental bio-geochemical process parameters in LandscapeDNDC when simulation

742   soil C and N fluxes. Propagating these joint parameter distributions through the model (by

743   sampling 500 joint parameter distributions and performing inventory simulations with each

744   parameter set with the model) for estimating the regional C and N fluxes was leading to various

745   distributions for any model result on the regional scale. Statistical analysis calculating mean,

746   median as well as the interquartile range (Q25 to Q75) determines best estimates and the

747   uncertainty range of any model output on the regional scale, demonstrating the superiority of

748   the method for assessing any ecosystem response by modelling instead of reporting single

749   results. This is a novel approach, that to our knowledge has not been reported before in

750   literature for the full carbon and nitrogen balance and neither been applied to regional

751   simulations by any process-based model.

752   In this study, the estimated UA mean and median of the carbon sequestration of 0.5 ± 0.3 tons

753   C ha^{-1} yr^{-1} is associated with an uncertainty range from 0.4 to 0.7 tons C ha^{-1} yr^{-1} which

754   compares well to the spatial uncertainty of C-sequestration in the study of Haas et al., (2022).

755   The approach used in this study enabled to assess the carbon and nitrogen balance of the

756   Lehuger et al., (2009b) used the Bayesian calibration method for the enhancement of the

757   CERES-EGC model parameterization (reduction of the apriori parameter distribution) as well

758   as quantification of the uncertainty of the simulated N_2O emissions in different sites. The

759   estimated fluxes of the different sites resulted in a range between 0.088 to 3.672 kg N_2O-N ha^{-1}

760   yr^{-1} with values for the q05 quantile of 0.066 to 0.115 kg N_2O-N ha^{-1} yr^{-1} and for the Q95

761   quantile from 1.676 to 5.874 kg N_2O-N ha^{-1} yr^{-1} with an averaged value of 1.04 kg N_2O-N ha^{-1}

762   yr^{-1} which is lower than the result of the current study but still in the same order of magnitude.

763   Klatt et al., (2015b) quantified a parameter-induced uncertainty analysis on the regional scale

764   applying the same process model for simulating N_2O emission and NO_3 leaching inventories

765   similar to our study. The region was represented by 4000 polygons of arable land (state of

766   Saxony, Germany) for crop rotations of barley, wheat and rapeseed while climatic conditions

767   differ. The results of Klatt et al., (2015b) display a likelihood range of 50% (the IQR range

768   between Q25 and Q75) for N_2O emissions from 0.46 to 2.05 kg N_2O-N ha^{-1} yr^{-1} which is in

769   good comparison to our results of 2.1 to 3.1 kg N_2O-N ha^{-1} yr^{-1}. The average N_2O emissions

770   are 1.43 kg N_2O-N ha^{-1} yr^{-1} comparable to the result of our study (mean: 2.6 and median: 2.5

771   kg N_2O-N ha^{-1} yr^{-1} across approx. 1000 polygons). As for leached NO_3, Klatt et al., (2015b)

772   reported leaching rates of mean value: 29 kg NO_3-N ha^{-1} yr^{-1}, (IQR from 24.5 to 36.0), which

773   is higher compared to the results of our study: Mean: 14.1 kg NO_3-N ha^{-1} yr^{-1}, median: 13.6

774   kg NO_3-N ha^{-1} yr^{-1} (IQR from 11 to 17). Despite the difference in climatic and soil conditions,

775 both uncertainty analysis studies reported similar regional estimates and uncertainty ranges

776 for N_2O emissions and NO_3 leaching.

777 Butterbach-Bahl et al., (2022) reported the influence of management uncertainties for

778 compiling national inventories of CH_4 and N_2O emission from various rice cultivation systems

779 in Vietnam. The study applied a sampling technique varying model input data within a given

780 range and analysing the influence on the assessed CH_4 and N_2O emission strengths. As the

781 underlying cropland systems were fundamentally different, the assessed uncertainty ranges

782 were comparable and the study is supporting our approach to focus on reporting uncertainty

783 ranges rather than single values.

784

785 5   Conclusion

786

787 In this research, we presented for the first time a regional inventory of the full carbon and

788 nitrogen balance including all sub-components of these fluxes simulated by a process-based

789 model. Additionally, the study has fulfilled the demand to report always the associated

790 uncertainties for any modelling results being published in literature. This supports the

791 trustworthiness of the reported results for the C and N balances.

792 Comparing the modelled N balance with a similar approach modelling the full N balance with

793 all associated fluxes for a catchment in pre-alpine Austria leads to the conclusion, that

794 especially the partitioning the N outflux into the different N flux components is more inherent

795 to the LandscapeDNDC model itself used in both studies than induced by the two very different

796 agricultural and climatical systems. Nevertheless, specific N outfluxes between the two studies

797 show large differences (e.g. NH_3 volatilization), which is purely caused by model processes

798 due to different soil PH values. Comparing to a less granular and detailed study of the N

799 balance for Switzerland gives a first impressions of the differences to be expected in modelling

800 the arable N balance with various different models. The discussion of such results will become

801 more lively and maybe controversial as soon as more comparable studies using different

802 models become available.

803 In addition, a full uncertainty analysis is presented based on the Metropolis-Hastings algorithm

804 where a parameter subset and input data perturbation was sampled and simulated resulting in

805 various probability density functions (PDF) for each one of the N and C balance fluxes building

806 a full uncertainty analysis of the modelled results. This helps to build trustworthiness in

807 modelling assessments and estimates of the balances as well as of the model behaviour.

808 As demanded by the nitrogen modelling community, all of the above constitute the novelty of

809 the conducted research that could be seen as a prototype to analyse and report N cycling in

810 agro-ecosystems in the future.

811

812 6   Aknowledgements

813 The author Odysseas Sifounakis received a Ph.D. research scholarship from Alexandros S.

814 Onassis Public Benefit Foundation, Greece, part of which is the research presented in the

815 current publication.

816

817 7   Code/Data availability

818 The LandscapeDNDC model source code is available via Butterbach-Bahl, Klaus; Grote,

819 Rüdiger; Haas, Edwin; et al. (2021): LandscapeDNDC (v1.30.4). Karlsruhe Institute of

820 Technology (KIT). DOI: 10.35097/438

821 All publication results (tables and data for figures) will be made available in the supplementary

822 material associated with this paper.

823

824

8 Author contributions

Mr. Odysseas Sifounakis has conceived and designed the analysis and collected the data. He, also, performed the analysis and wrote the paper.

Dr. Edwin Haas conducted research and wrote the paper.

Prof. Dr. Klaus Butterbach-Bahl substantially contributed to research planning, manuscript writing and editing and, also, provided funding opportunities.

Prof. Dr. Maria P. Papadopoulou substantially contributed to research planning, manuscript writing and editing, and provided funding opportunities.

9 Competing interests

All authors have reviewed and accepted the submitted version and declare no conflicts of interest related to this publication.

10 References

Barneze, A.S., Whitaker, J., McNamara, N.P., Ostle, N.J., 2020. Legumes increase grassland productivity with no effect on nitrous oxide emissions. Plant Soil 446, 163–177. https://doi.org/10.1007/s11104-019-04338-w

Butterbach-Bahl, K., Baggs, E.M., Dannenmann, M., Kiese, R., Zechmeister-Boltenstern, S., 2013. Nitrous oxide emissions from soils: How well do we understand the processes and their controls? Philosophical Transactions of the Royal Society B: Biological Sciences. https://doi.org/10.1098/rstb.2013.0122

Butterbach-Bahl, K., Kahl, M., Mykhayliv, L., Werner, C., Kiese, R., Li, C., 2009. A European-wide inventory of soil NO emissions using the biogeochemical models DNDC/Forest-DNDC. Atmos Environ 43, 1392–1402. https://doi.org/10.1016/J.ATMOSENV.2008.02.008

Butterbach-Bahl, K., Kraus, D., Kiese, R., Mai, V.T., Nguyen, T., Sander, B.O., Wassmann, R., Werner, C., 2022. Activity data on crop management define uncertainty of CH_4 and N_2

852   O emission estimates from rice: A case study of Vietnam . Journal of Plant Nutrition and

853   Soil Science. https://doi.org/10.1002/jpln.202200382

854 Camargo, J.A., Alonso, Á., 2006. Ecological and toxicological effects of inorganic nitrogen

855   pollution in aquatic ecosystems: A global assessment. Environ Int.

856   https://doi.org/10.1016/j.envint.2006.05.002

857 Cameron, D.R., van Oijen, M., Werner, C., Butterbach-Bahl, K., Grote, R., Haas, E., Heuvelink,

858   G.B.M., Kiese, R., Kros, J., Kuhnert, M., Leip, A., Reinds, G.J., Reuter, H.I., Schelhaas,

859   M.J., de Vries, W., Yeluripati, J., 2013. Environmental change impacts on the C- and N-

860   cycle of European forests: A model comparison study. Biogeosciences 10, 1751–1773.

861   https://doi.org/10.5194/bg-10-1751-2013

862 Cayuela, M.L., Aguilera, E., Sanz-Cobena, A., Adams, D.C., Abalos, D., Barton, L., Ryals, R.,

863   Silver, W.L., Alfaro, M.A., Pappa, V.A., Smith, P., Garnier, J., Billen, G., Bouwman, L.,

864   Bondeau, A., Lassaletta, L., 2017. Direct nitrous oxide emissions in Mediterranean

865   climate cropping systems: Emission factors based on a meta-analysis of available

866   measurement data. Agric Ecosyst Environ 238, 25–35.

867   https://doi.org/10.1016/j.agee.2016.10.006

868 Chirinda, N., Kracher, D., Lægdsmand, M., Porter, J.R., Olesen, J.E., Petersen, B.M., Doltra,

869   J., Kiese, R., Butterbach-Bahl, K., 2011. Simulating soil N2O emissions and heterotrophic

870   CO2 respiration in arable systems using FASSET and MoBiLE-DNDC. Plant Soil 343,

871   139–160. https://doi.org/10.1007/s11104-010-0596-7

872 Ciais, P., Wattenbach, M., Vuichard, N., Smith, P., Piao, S.L., Don, A., Luyssaert, S.,

873   Janssens, I.A., Bondeau, A., Dechow, R., Leip, A., Smith, P.C., Beer, C., van der werf,

874   G.R., Gervois, S., van oost, K., Tomelleri, E., Freibauer, A., Schulze, E.D., 2010a. The

875   European carbon balance. Part 2: Croplands. Glob Chang Biol 16, 1409–1428.

876   https://doi.org/10.1111/j.1365-2486.2009.02055.x

877 Ciais, P., Wattenbach, M., Vuichard, N., Smith, P., Piao, S.L., Don, A., Luyssaert, S.,

878   Janssens, I.A., Bondeau, A., Dechow, R., Leip, A., Smith, P.C., Beer, C., van der werf,

879   G.R., Gervois, S., van oost, K., Tomelleri, E., Freibauer, A., Schulze, E.D., 2010b. The

880   European carbon balance. Part 2: Croplands. Glob Chang Biol 16, 1409–1428.

881   https://doi.org/10.1111/j.1365-2486.2009.02055.x

882   Dambreville, C., Morvan, T., Germon, J.C., 2008. N2O emission in maize-crops fertilized with

883   pig slurry, matured pig manure or ammonium nitrate in Brittany. Agric Ecosyst Environ

884   123, 201–210. https://doi.org/10.1016/j.agee.2007.06.001

885   Davidson, E.A., Kanter, D., 2014. Inventories and scenarios of nitrous oxide emissions.

886   Environmental Research Letters 9. https://doi.org/10.1088/1748-9326/9/10/105012

887   de Vries, W., Leip, A., Reinds, G.J., Kros, J., Lesschen, J.P., Bouwman, A.F., 2011.

888   Comparison of land nitrogen budgets for European agriculture by various modeling

889   approaches. Environmental Pollution 159, 3254–3268.

890   https://doi.org/10.1016/j.envpol.2011.03.038

891   del Grosso, S.J., Mosier, A.R., Parton, W.J., Ojima, D.S., 2005. DAYCENT model analysis of

892   past and contemporary soil N2O and net greenhouse gas flux for major crops in the USA.

893   Soil Tillage Res 83, 9–24. https://doi.org/10.1016/J.STILL.2005.02.007

894   del Grosso, S.J., Ogle, S.M., Nevison, C., Gurung, R., Parton, W.J., Wagner-Riddle, C., Smith,

895   W., Winiwarter, W., Grant, B., Tenuta, M., Marx, E., Spencer, S., Williams, S., 2022. A

896   gap in nitrous oxide emission reporting complicates long-term climate mitigation. Proc

897   Natl Acad Sci U S A 119. https://doi.org/10.1073/pnas.2200354119

898   del Grosso, S.J., Ojima, D.S., Parton, W.J., Stehfest, E., Heistemann, M., DeAngelo, B., Rose,

899   S., 2009. Global scale DAYCENT model analysis of greenhouse gas emissions and

900   mitigation strategies for cropped soils. Glob Planet Change 67, 44–50.

901   https://doi.org/10.1016/J.GLOPLACHA.2008.12.006

902   EFMA, 2009. SUSTAINABLE AGRICULTURE IN EUROPE.

903   Erisman, J.W., Galloway, J., Seitzinger, S., Bleeker, A., Butterbach-Bahl, K., 2011. Reactive

904   nitrogen in the environment and its effect on climate change. Curr Opin Environ Sustain

905   3, 281–290. https://doi.org/10.1016/J.COSUST.2011.08.012

906 ESDB, 2004. European Soil Database (ESDB) v2.0 - raster version [WWW Document]. URL
907   https://esdac.jrc.ec.europa.eu/ESDB_Archive/ESDB/ESDB_Data/ESDB_v2_data_smu_
908   1k.html (accessed 1.13.19).

909 EU-Commission, 2019. European Commission-Press release Nitrates: Commission decides
910   to refer Greece to the Court of Justice and asks for financial sanctions.

911 EU-Commission, 2014. Tracking progress towards Kyoto and 2020 targets in Europe —
912   European Environment Agency [WWW Document]. URL
913   https://www.eea.europa.eu/publications/progress-towards-kyoto (accessed 1.13.19).

914 Franke, J.A., Müller, C., Elliott, J., Ruane, A.C., Jägermeyr, J., Balkovic, J., Ciais, P., Dury, M.,
915   Falloon, P.D., Folberth, C., François, L., Hank, T., Hoffmann, M., Izaurralde, R.C.,
916   Jacquemin, I., Jones, C., Khabarov, N., Koch, M., Li, M., Liu, W., Olin, S., Phillips, M.,
917   Pugh, T.A.M., Reddy, A., Wang, X., Williams, K., Zabel, F., Moyer, E.J., 2020. The
918   GGCMI Phase 2 experiment: Global gridded crop model simulations under uniform
919   changes in CO_2, temperature, water, and nitrogen levels (protocol version 1.0). Geosci
920   Model Dev 13, 2315–2336. https://doi.org/10.5194/gmd-13-2315-2020

921 Fuchs, K., Merbold, L., Buchmann, N., Bretscher, D., Brilli, L., Fitton, N., Topp, C.F.E., Klumpp,
922   K., Lieffering, M., Martin, R., Newton, P.C.D., Rees, R.M., Rolinski, S., Smith, P., Snow,
923   V., 2020. Multimodel Evaluation of Nitrous Oxide Emissions From an Intensively
924   Managed Grassland. J Geophys Res Biogeosci 125.
925   https://doi.org/10.1029/2019JG005261

926 Gabrielle, B., Laville, P., Hénault, C., Nicoullaud, B., Germon, J.C., 2006. Simulation of nitrous
927   oxide emissions from wheat-cropped soils using CERES. Nutr Cycl Agroecosyst 74, 133–
928   146. https://doi.org/10.1007/s10705-005-5771-5

929 Galloway, J.N., Leach, A.M., Bleeker, A., Erisman, J.W., 2013. A chronology of human
930   understanding of the nitrogen cycle. Philosophical Transactions of the Royal Society B:
931   Biological Sciences. https://doi.org/10.1098/rstb.2013.0120

932 Garnett, T., Appleby, M.C., Balmford, A., Bateman, I.J., Benton, T.G., Bloomer, P., Burlingame,
933   B., Dawkins, M., Dolan, L., Fraser, D., Herrero, M., Hoffmann, I., Smith, P., Thornton,

934   P.K., Toulmin, C., Vermeulen, S.J., Godfray, H.C.J., 2013. Sustainable intensification in

935   agriculture: Premises and policies. Science (1979).

936   https://doi.org/10.1126/science.1234485

937 Geels, C., Andersen, H. v., Ambelas Skjøth, C., Christensen, J.H., Ellermann, T., Løfstrøm,

938   P., Gyldenkærne, S., Brandt, J., Hansen, K.M., Frohn, L.M., Hertel, O., 2012. Improved

939   modelling of atmospheric ammonia over Denmark using the coupled modelling system

940   DAMOS. Biogeosciences 9, 2625–2647. https://doi.org/10.5194/bg-9-2625-2012

941 Godfray, H.C.J., Beddington, J.R., Crute, I.R., Haddad, L., Lawrence, D., Muir, J.F., Pretty, J.,

942   Robinson, S., Thomas, S.M., Toulmin, C., 2010. Food security: The challenge of feeding

943   9 billion people. Science (1979). https://doi.org/10.1126/science.1185383

944 Grosz, B., Matson, A., Butterbach-Bah, K., Clough, T., Davidson, E.A., Dechow, R.,

945   Diamantopoulos, E., Dörsch, P., Haas, E., He, H., Henri, C. V, Hui, D., Well, R., Yeluripati,

946   J., Zhang, J., Scheer, C., 2023. Modeling denitrification: can we report what we don't

947   know? ESS Open Archive. https://doi.org/10.22541/essoar.168500283.32887682/v1

948 Grote, R., Lehmann, E., Brümmer, C., Brüggemann, N., Szarzynski, J., Kunstmann, H., 2009.

949   Modelling and observation of biosphere–atmosphere interactions in natural savannah in

950   Burkina Faso, West Africa. Physics and Chemistry of the Earth, Parts A/B/C 34, 251–260.

951   https://doi.org/10.1016/J.PCE.2008.05.003

952 Gurung, R.B., Ogle, S.M., Breidt, F.J., Williams, S.A., Parton, W.J., 2020. Bayesian calibration

953   of the DayCent ecosystem model to simulate soil organic carbon dynamics and reduce

954   model uncertainty. Geoderma 376. https://doi.org/10.1016/j.geoderma.2020.114529

955 Haas, E., Carozzi, M., Massad, R.S., Butterbach-Bahl, K., Scheer, C., 2022. Long term impact

956   of residue management on soil organic carbon stocks and nitrous oxide emissions from

957   European croplands. Science of The Total Environment 836, 154932.

958   https://doi.org/10.1016/J.SCITOTENV.2022.154932

959 Haas, E., Klatt, S., Fröhlich, A., Kraft, P., Werner, C., Kiese, R., Grote, R., Breuer, L.,

960   Butterbach-Bahl, K., 2013. LandscapeDNDC: A process model for simulation of

biosphere-atmosphere-hydrosphere exchange processes at site and regional scale. Landsc Ecol 28, 615–636. https://doi.org/10.1007/s10980-012-9772-x

He, W., Jiang, R., He, P., Yang, J., Zhou, W., Ma, J., Liu, Y., 2018. Estimating soil nitrogen balance at regional scale in China's croplands from 1984 to 2014. Agric Syst 167, 125–135. https://doi.org/10.1016/J.AGSY.2018.09.002

Heinen, M., 2006. Application of a widely used denitrification model to Dutch data sets. Geoderma 133, 464–473. https://doi.org/10.1016/J.GEODERMA.2005.08.011

Hénault, C., Bizouard, F., Laville, P., Gabrielle, B., Nicoullaud, B., Germon, J.C., Cellier, P., 2005. Predicting in situ soil N2O emission using NOE algorithm and soil database. Glob Chang Biol 11, 115–127. https://doi.org/10.1111/j.1365-2486.2004.00879.x

Holst, J., Grote, R., Offermann, C., Ferrio, J.P., Gessler, A., Mayer, H., Rennenberg, H., 2010. Water fluxes within beech stands in complex terrain. Int J Biometeorol 54, 23–36. https://doi.org/10.1007/s00484-009-0248-x

Houska, T., Kraft, P., Liebermann, R., Klatt, S., Kraus, D., Haas, E., Santabarbara, I., Kiese, R., Butterbach-Bahl, K., Müller, C., Breuer, L., 2017. Rejecting hydro-biogeochemical model structures by multi-criteria evaluation. Environmental Modelling and Software 93, 1–12. https://doi.org/10.1016/j.envsoft.2017.03.005

IFADATA [WWW Document], 2015. URL http://ifadata.fertilizer.org/ucSearch.aspx (accessed 1.13.19).

IPCC, 2019. 2019 Refinement to the 2006 IPCC Guidelines for National Greenhouse Gas Inventories — IPCC [WWW Document]. URL https://www.ipcc.ch/report/2019-refinement-to-the-2006-ipcc-guidelines-for-national-greenhouse-gas-inventories/ (accessed 1.12.19).

Jägermeyr, J., Müller, C., Ruane, A.C., Elliott, J., Balkovic, J., Castillo, O., Faye, B., Foster, I., Folberth, C., Franke, J.A., Fuchs, K., Guarin, J.R., Heinke, J., Hoogenboom, G., Iizumi, T., Jain, A.K., Kelly, D., Khabarov, N., Lange, S., Lin, T.S., Liu, W., Mialyk, O., Minoli, S., Moyer, E.J., Okada, M., Phillips, M., Porter, C., Rabin, S.S., Scheer, C., Schneider, J.M., Schyns, J.F., Skalsky, R., Smerald, A., Stella, T., Stephens, H., Webber, H., Zabel, F.,

989   Rosenzweig, C., 2021. Climate impacts on global agriculture emerge earlier in new

990   generation of climate and crop models. Nat Food 2, 873–885.

991   https://doi.org/10.1038/s43016-021-00400-y

992 Janz, B., Havermann, F., Lashermes, G., Zuazo, P., Engelsberger, F., Torabi, S.M.,

993   Butterbach-Bahl, K., 2022. Effects of crop residue incorporation and properties on

994   combined soil gaseous N2O, NO, and NH3 emissions—A laboratory-based measurement

995   approach. Science of The Total Environment 807, 151051.

996   https://doi.org/10.1016/J.SCITOTENV.2021.151051

997 Jones, C.M., Spor, A., Brennan, F.P., Breuil, M.C., Bru, D., Lemanceau, P., Griffiths, B., Hallin,

998   S., Philippot, L., 2014. Recently identified microbial guild mediates soil N2O sink capacity.

999   Nat Clim Chang 4, 801–805. https://doi.org/10.1038/nclimate2301

1000 Kalivas, D., Kollias, V., Kalivas, D.P., Kollias, V.J., 2001. Effects of soil, climate and cultivation

1001   techniques on cotton yield in Central Greece, using different statistical methods 21.

1002   https://doi.org/10.1051/agro:2001110ï

1003 Kasper, M., Foldal, C., Kitzler, B., Haas, E., Strauss, P., Eder, A., Zechmeister-Boltenstern,

1004   S., Amon, B., 2019. N 2 O emissions and NO 3− leaching from two contrasting regions in

1005   Austria and influence of soil, crops and climate: a modelling approach. Nutr Cycl

1006   Agroecosyst 113, 95–111. https://doi.org/10.1007/s10705-018-9965-z

1007 Kim, Y., Seo, Y., Kraus, D., Klatt, S., Haas, E., Tenhunen, J., Kiese, R., 2015. Estimation and

1008   mitigation of N2O emission and nitrate leaching from intensive crop cultivation in the

1009   Haean catchment, South Korea. Science of The Total Environment 529, 40–53.

1010   https://doi.org/10.1016/J.SCITOTENV.2015.04.098

1011 Klatt, S., Kraus, D., Rahn, K.-H., Werner, C., Kiese, R., Butterbach-Bahl, K., Haas, E., 2015a.

1012   Parameter-Induced Uncertainty Quantification of Regional N 2 O Emissions and NO 3

1013   Leaching using the Biogeochemical Model LandscapeDNDC . pp. 149–171.

1014   https://doi.org/10.2134/advagricsystmodel6.2013.0001

1015 Klatt, S., Kraus, D., Rahn, K.-H., Werner, C., Kiese, R., Butterbach-Bahl, K., Haas, E., 2015b.

1016   Parameter-Induced Uncertainty Quantification of Regional N 2 O Emissions and NO 3

Leaching using the Biogeochemical Model LandscapeDNDC . pp. 149–171. https://doi.org/10.2134/advagricsystmodel6.2013.0001

Kraus, D., Weller, S., Klatt, S., Haas, E., Wassmann, R., Kiese, R., Butterbach-Bahl, K., 2014. A new LandscapeDNDC biogeochemical module to predict CH4 and N2O emissions from lowland rice and upland cropping systems. Plant Soil 386, 125–149. https://doi.org/10.1007/s11104-014-2255-x

Larocque, G.R., Bhatti, J.S., Boutin, R., Chertov, O., 2008. Uncertainty analysis in carbon cycle models of forest ecosystems: Research needs and development of a theoretical framework to estimate error propagation. Ecol Modell 219, 400–412. https://doi.org/10.1016/J.ECOLMODEL.2008.07.024

Lee, K.M., Lee, M.H., Lee, J.S., Lee, J.Y., 2020. Uncertainty analysis of greenhouse gas (GHG) emissions simulated by the parametric Monte Carlo simulation and nonparametric bootstrap method. Energies (Basel) 13. https://doi.org/10.3390/en13184965

Lehuger, S., Gabrielle, B., Oijen, M. van, Makowski, D., Germon, J.C., Morvan, T., Hénault, C., 2009a. Bayesian calibration of the nitrous oxide emission module of an agro-ecosystem model. Agric Ecosyst Environ 133, 208–222. https://doi.org/10.1016/j.agee.2009.04.022

Lehuger, S., Gabrielle, B., Oijen, M. van, Makowski, D., Germon, J.C., Morvan, T., Hénault, C., 2009b. Bayesian calibration of the nitrous oxide emission module of an agro-ecosystem model. Agric Ecosyst Environ 133, 208–222. https://doi.org/10.1016/J.AGEE.2009.04.022

Leip, A., Busto, M., Corazza, M., Bergamaschi, P., Koeble, R., Dechow, R., Monni, S., de Vries, W., 2011. Estimation of N 2O fluxes at the regional scale: Data, models, challenges. Curr Opin Environ Sustain. https://doi.org/10.1016/j.cosust.2011.07.002

Li, C.S., 2000. Modeling trace gas emissions from agricultural ecosystems. Nutr Cycl Agroecosyst 58, 259–276.

Li, X., Yeluripati, J., Jones, E.O., Uchida, Y., Hatano, R., 2015. Hierarchical Bayesian calibration of nitrous oxide (N2O) and nitrogen monoxide (NO) flux module of an agro-

1045   ecosystem model: ECOSSE. Ecol Modell 316, 14–27.

1046   https://doi.org/10.1016/J.ECOLMODEL.2015.07.020

1047   Lu, X., 2020. A meta-analysis of the effects of crop residue return on crop yields and water use

1048   efficiency. PLoS One 15. https://doi.org/10.1371/journal.pone.0231740

1049   Lugato, E., Bampa, F., Panagos, P., Montanarella, L., Jones, A., 2014. Potential carbon

1050   sequestration of European arable soils estimated by modelling a comprehensive set of

1051   management practices. Glob Chang Biol 20, 3557–3567.

1052   https://doi.org/10.1111/gcb.12551

1053   Lugato, E., Leip, A., Jones, A., 2018. Mitigation potential of soil carbon management

1054   overestimated by neglecting N_2O emissions. Nat Clim Chang 8, 219–223.

1055   https://doi.org/10.1038/s41558-018-0087-z

1056   Lyra, A., Loukas, A., 2021. Impacts of irrigation and nitrate fertilization scenarios on

1057   groundwater resources quantity and quality of the Almyros Basin, Greece. Water Supply

1058   21, 2748–2759. https://doi.org/10.2166/ws.2021.097

1059   Mavromatis, T., 2016. Spatial resolution effects on crop yield forecasts: An application to

1060   rainfed wheat yield in north Greece with CERES-Wheat. Agric Syst 143, 38–48.

1061   https://doi.org/10.1016/j.agsy.2015.12.002

1062   Molina-Herrera, S., Grote, R., Santabárbara-Ruiz, I., Kraus, D., Klatt, S., Haas, E., Kiese, R.,

1063   Butterbach-Bahl, K., 2015. Simulation of CO_2 fluxes in European forest ecosystems with

1064   the coupled soil-vegetation process model "LandscapeDNDC." Forests 6, 1779–1809.

1065   https://doi.org/10.3390/f6061779

1066   Molina-Herrera, S., Haas, E., Grote, R., Kiese, R., Klatt, S., Kraus, D., Butterbach-Bahl, K.,

1067   Kampffmeyer, T., Friedrich, R., Andreae, H., Loubet, B., Ammann, C., Horváth, L., Larsen,

1068   K., Gruening, C., Frumau, A., Butterbach-Bahl, K., 2017. Importance of soil NO emissions

1069   for the total atmospheric NOx budget of Saxony, Germany. Atmos Environ 152, 61–76.

1070   https://doi.org/10.1016/J.ATMOSENV.2016.12.022

1071   Molina-Herrera, S., Haas, E., Klatt, S., Kraus, D., Augustin, J., Magliulo, V., Tallec, T., Ceschia,

1072   E., Ammann, C., Loubet, B., Skiba, U., Jones, S., Brümmer, C., Butterbach-Bahl, K.,

Kiese, R., 2016. A modeling study on mitigation of N2O emissions and NO3 leaching at different agricultural sites across Europe using LandscapeDNDC. Science of the Total Environment 553, 128–140. https://doi.org/10.1016/j.scitotenv.2015.12.099

Morris, M.D., 1991. Factorial Sampling Plans for Preliminary Computational Experiments, TECHNOMETRICS.

Musacchio, A., Re, V., Mas-Pla, J., Sacchi, E., 2020. EU Nitrates Directive, from theory to practice: Environmental effectiveness and influence of regional governance on its performance. Ambio 49, 504–516. https://doi.org/10.1007/s13280-019-01197-8

Myrgiotis, V., Rees, R.M., Topp, C.F.E., Williams, M., 2018a. A systematic approach to identifying key parameters and processes in agroecosystem models. Ecol Modell 368, 344–356. https://doi.org/10.1016/j.ecolmodel.2017.12.009

Myrgiotis, V., Williams, M., Rees, R.M., Topp, C.F.E., 2019. Estimating the soil N2O emission intensity of croplands in northwest Europe. Biogeosciences 16, 1641–1655. https://doi.org/10.5194/bg-16-1641-2019

Myrgiotis, V., Williams, M., Topp, C.F.E., Rees, R.M., 2018b. Improving model prediction of soil N2O emissions through Bayesian calibration. Science of the Total Environment 624, 1467–1477. https://doi.org/10.1016/j.scitotenv.2017.12.202

OECD, 2020. OECD (2020), Nutrient balance (indicator) [WWW Document]. URL https://data.oecd.org/agrland/nutrient-balance.htm (accessed 2.16.20).

Petersen, K., Kraus, D., Calanca, P., Semenov, M.A., Butterbach-Bahl, K., Kiese, R., 2021. Dynamic simulation of management events for assessing impacts of climate change on pre-alpine grassland productivity. European Journal of Agronomy 128, 126306. https://doi.org/10.1016/J.EJA.2021.126306

Petersen, R.J., Blicher-Mathiesen, G., Rolighed, J., Andersen, H.E., Kronvang, B., 2021. Three decades of regulation of agricultural nitrogen losses: Experiences from the Danish Agricultural Monitoring Program. Science of The Total Environment 787, 147619. https://doi.org/10.1016/J.SCITOTENV.2021.147619

Portmann, F.T., Siebert, S., Döll, P., 2010. MIRCA2000-Global monthly irrigated and rainfed crop areas around the year 2000: A new high-resolution data set for agricultural and hydrological modeling. Global Biogeochem Cycles 24, n/a-n/a. https://doi.org/10.1029/2008gb003435

Rahn, K.H., Werner, C., Kiese, R., Haas, E., Butterbach-Bahl, K., 2012. Parameter-induced uncertainty quantification of soil N_2O, NO and CO_2 emission from Höglwald spruce forest (Germany) using the LandscapeDNDC model. Biogeosciences 9, 3983–3998. https://doi.org/10.5194/bg-9-3983-2012

Ramanantenasoa, M.M.J., Gilliot, J.M., Mignolet, C., Bedos, C., Mathias, E., Eglin, T., Makowski, D., Génermont, S., 2018. A new framework to estimate spatio-temporal ammonia emissions due to nitrogen fertilization in France. Science of The Total Environment 645, 205–219. https://doi.org/10.1016/J.SCITOTENV.2018.06.202

Ranucci, S., Bertolini, T., Vitale, L., di Tommasi, P., Ottaiano, L., Oliva, M., Amato, U., Fierro, A., Magliulo, V., 2011. The influence of management and environmental variables on soil N2O emissions in a crop system in Southern Italy. Plant Soil 343, 83–96. https://doi.org/10.1007/s11104-010-0674-x

Ravishankara, A.R., Daniel, J.S., Portmann, R.W., 2009. Nitrous oxide (N2O): The dominant ozone-depleting substance emitted in the 21st century. Science (1979) 326, 123–125. https://doi.org/10.1126/science.1176985

Refsgaard, J.C., van der Sluijs, J.P., Højberg, A.L., Vanrolleghem, P.A., 2007. Uncertainty in the environmental modelling process – A framework and guidance. Environmental Modelling & Software 22, 1543–1556. https://doi.org/10.1016/J.ENVSOFT.2007.02.004

Robert, C., Casella, G., 2011. A short history of Markov Chain Monte Carlo: Subjective recollections from incomplete data. Statistical Science 26, 102–115. https://doi.org/10.1214/10-STS351

Salteli, A., Tarantola, S., Campolongo, F., 2000. Sensitivity Analysis as an Ingredient of Modeling. Statistical Science 15, 377–395.

Santabárbara, I., 2019. Analysis and quantification of parametric and structural uncertainty of the LandscapeDNDC model for simulating biosphere-atmosphere-hydrosphere exchange processes.

Schroeck, A.M., Gaube, V., Haas, E., Winiwarter, W., 2019. Estimating nitrogen flows of agricultural soils at a landscape level – A modelling study of the Upper Enns Valley, a long-term socio-ecological research region in Austria. Science of the Total Environment 665, 275–289. https://doi.org/10.1016/j.scitotenv.2019.02.071

Sidiropoulos, C., Tsilingiridis, G., 2009. Trends of livestock-related NH_3, CH_4, N_2O and PM emissions in Greece. Water Air Soil Pollut 199, 277–289. https://doi.org/10.1007/s11270-008-9877-7

Smerald, A., Fuchs, K., Kraus, D., Butterbach-Bahl, K., Scheer, C., 2022. Significant Global Yield-Gap Closing Is Possible Without Increasing the Intensity of Environmentally Harmful Nitrogen Losses. Front Sustain Food Syst 6. https://doi.org/10.3389/fsufs.2022.736394

Smith, P., Martino, D., Cai, Z., Gwary, D., Janzen, H., Kumar, P., McCarl, B., Ogle, S., O'Mara, F., Rice, C., Scholes, B., Sirotenko, O., Howden, M., McAllister, T., Pan, G., Romanenkov, V., Schneider, U., Towprayoon, S., Wattenbach, M., Smith, J., 2008. Greenhouse gas mitigation in agriculture. Philosophical Transactions of the Royal Society B: Biological Sciences. https://doi.org/10.1098/rstb.2007.2184

Stehfest, E., Bouwman, L., 2006. N_2O and NO emission from agricultural fields and soils under natural vegetation: Summarizing available measurement data and modeling of global annual emissions. Nutr Cycl Agroecosyst 74, 207–228. https://doi.org/10.1007/s10705-006-9000-7

Sutton, M.A., Reis, S., Riddick, S.N., Dragosits, U., Nemitz, E., Theobald, M.R., Tang, Y.S., Braban, C.F., Vieno, M., Dore, A.J., Mitchell, R.F., Wanless, S., Daunt, F., Fowler, D., Blackall, T.D., Milford, C., Flechard, C.R., Loubet, B., Massad, R., Cellier, P., Personne, E., Coheur, P.F., Clarisse, L., van Damme, M., Ngadi, Y., Clerbaux, C., Skjøth, C.A., Geels, C., Hertel, O., Kruit, R.J.W., Pinder, R.W., Bash, J.O., Walker, J.T., Simpson, D., Horváth, L., Misselbrook, T.H., Bleeker, A., Dentener, F., de Vries, W., 2013. Towards a

climate-dependent paradigm of ammonia emission and deposition. Philosophical Transactions of the Royal Society B: Biological Sciences 368. https://doi.org/10.1098/rstb.2013.0166

Thomas, D., Johannes, K., David, K., Rüdiger, G., Ralf, K., 2016. Impacts of management and climate change on nitrate leaching in a forested karst area. J Environ Manage 165, 243–252. https://doi.org/10.1016/J.JENVMAN.2015.09.039

Thompson, R.L., Lassaletta, L., Patra, P.K., Wilson, C., Wells, K.C., Gressent, A., Koffi, E.N., Chipperfield, M.P., Winiwarter, W., Davidson, E.A., Tian, H., Canadell, J.G., 2019. Acceleration of global N2O emissions seen from two decades of atmospheric inversion. Nat Clim Chang 9, 993–998. https://doi.org/10.1038/s41558-019-0613-7

Tsakmakis, I.D., Kokkos, N.P., Gikas, G.D., Pisinaras, V., Hatzigiannakis, E., Arampatzis, G., Sylaios, G.K., 2019. Evaluation of AquaCrop model simulations of cotton growth under deficit irrigation with an emphasis on root growth and water extraction patterns. Agric Water Manag 213, 419–432. https://doi.org/10.1016/j.agwat.2018.10.029

Velthof, G.L., Oudendag, D., Witzke, H.P., Asman, W.A.H., Klimont, Z., Oenema, O., 2009. Integrated Assessment of Nitrogen Losses from Agriculture in EU-27 using MITERRA-EUROPE. J Environ Qual 38, 402–417. https://doi.org/10.2134/jeq2008.0108

Velthof, G.L., van Bruggen, C., Groenestein, C.M., de Haan, B.J., Hoogeveen, M.W., Huijsmans, J.F.M., 2012. A model for inventory of ammonia emissions from agriculture in the Netherlands. Atmos Environ 46, 248–255. https://doi.org/10.1016/J.ATMOSENV.2011.09.075

Vogeler, I., Giltrap, D., Cichota, R., 2013. Comparison of APSIM and DNDC simulations of nitrogen transformations and N2O emissions. Science of the Total Environment 465, 147–155. https://doi.org/10.1016/j.scitotenv.2012.09.021

Voloudakis, D., Karamanos, A., Economou, G., Kalivas, D., Vahamidis, P., Kotoulas, V., Kapsomenakis, J., Zerefos, C., 2015. Prediction of climate change impacts on cotton yields in Greece under eight climatic models using the AquaCrop crop simulation model

1182 and discriminant function analysis. Agric Water Manag 147, 116–128.

1183 https://doi.org/10.1016/j.agwat.2014.07.028

1184 Wagner-Riddle, C., Congreves, K.A., Abalos, D., Berg, A.A., Brown, S.E., Ambadan, J.T., Gao,

1185 X., Tenuta, M., 2017. Globally important nitrous oxide emissions from croplands induced

1186 by freeze-thaw cycles. Nat Geosci 10, 279–283. https://doi.org/10.1038/ngeo2907

1187 Wang, G., Chen, S., 2012. A review on parameterization and uncertainty in modeling

1188 greenhouse gas emissions from soil. Geoderma 170, 206–216.

1189 https://doi.org/10.1016/J.GEODERMA.2011.11.009

1190 Werner, C., Haas, E., Grote, R., Gauder, M., Graeff-Hönninger, S., Claupein, W., Butterbach-

1191 Bahl, K., 2012. Biomass production potential from Populus short rotation systems in

1192 Romania. GCB Bioenergy 4, 642–653. https://doi.org/10.1111/j.1757-1707.2012.01180.x

1193 Zhang, W., Liu, C., Zheng, X., Zhou, Z., Cui, F., Zhu, B., Haas, E., Klatt, S., Butterbach-Bahl,

1194 K., Kiese, R., 2015. Comparison of the DNDC, LandscapeDNDC and IAP-N-GAS models

1195 for simulating nitrous oxide and nitric oxide emissions from the winter wheat–summer

1196 maize rotation system. Agric Syst 140, 1–10.

1197 https://doi.org/10.1016/J.AGSY.2015.08.003

1198 Zistl-Schlingmann, M., Kwatcho Kengdo, S., Kiese, R., Dannenmann, M., 2020. Management

1199 Intensity Controls Nitrogen-Use-Efficiency and Flows in Grasslands—A 15N Tracing

1200 Experiment. Agronomy 10, 606. https://doi.org/10.3390/agronomy10040606

1201

1202 11 Appendix

1203 11.1 Material and Methods

1204 **Sensitivity Index**

1205 In the first step, the Sensitivity Index algorithm (SI) (Pannell, 1997) was calculated for all

1206 process parameters by splitting the parameter ranges into 10 equidistant values from minimum

1207 to maximum and by rating SI values:

1208 $$SI = \frac{CUM_{max} - CUM_{min}}{CUM_{max}}$$

1209 where CUM_{max} and CUM_{min} are the maximum and minimum cumulative results of 10

1210 simulations. High SI values explain a high sensitivity of the underlying parameter with respect

1211 to the model results, whereas low values or even zero indicates low or no sensitivity.

1212

1213 11.2 Results

1214 *Table A 1. Observed yield rates in the region of Thessaly. Cotton yields are the cotton bolls, clover feed is the total*
1215 *harvested above ground biomass, for wheat and barley it is the grain yield, maize is accounted grain ear and the*
1216 *stems Source ELSTAT.*

Crop Yields [tons dry matter ha⁻¹]						
Crops	2012	2013	2014	2015	2016	Mean
Cotton	2.7	3.6	3.5	3.4	3.3	3.3
Clover	8.6	8.9	8.7	7.9	7.7	8.4
Wheat	3.3	3.3	3.3	3.7	3.6	3.4
Barley	3.2	3.2	3.2	3.5	3.5	3.3
Maize	10.9	12.1	12.3	12.7	12.1	12.0

1217

1218 *Table A 2. Crop rotation scenarios (R1 – R5) for the region of Thessaly where the crop abbreviations corn, wiwh,*
1219 *perg, cott and wbar refer to maize, winter wheat, clover (legume feed crops s.a. alfalfa or vetch), cotton and winter*
1220 *barley respectively.*

years	R1	R2	R3	R4	R5
2010	corn	wiwh	perg	cott	wbar
2011	wiwh	perg	cott	wbar	corn
2012	perg	cott	wbar	corn	wiwh
2013	cott	wbar	corn	wiwh	perg

2014	wbar	corn	wiwh	perg	cott
2015	corn	wiwh	perg	cott	wbar
2016	wiwh	perg	cott	wbar	corn

1221

1222 *Table A 3. Carbon Balance (totals) Summary of the Assessment and Uncertainty Analysis of the of cropland*
1223 *cultivation of the region of Thessaly, Greece, GPP gross primary productivity, TER terrestrial ecosystem respiration,*
1224 *Biomass export includes all C in yield, straw and feed exported from the fields, 360000 ha cropland.*

	Mean	Std	Median	Q25	Q75
	[mio. tons C yr^{-1}]	[mio. tons C yr^{-1}]	[mio. tons C yr^{-1}]	[mio. tons C yr^{-1}]	[mio. tons C yr^{-1}]
C-Inputs	4.51	0.20	4.45	4.36	4.69
C-Outputs	4.32	0.17	4.31	4.19	4.45
SOC-changes	0.19	0.11	0.20	0.14	0.27
Input fluxes					
GPP	4.25	0.20	4.21	4.11	4.42
C in manure	0.25	0.01	0.26	0.25	0.26
Output fluxes					
TER	3.08	0.16	3.06	2.97	3.20
Biomass export	1.24	0.05	1.24	1.21	1.27

1225

1226 *Table A 4 Nitrogen balance (totals) Summary of the Assessment and Uncertainty Analysis of the total Nitrogen*
1227 *Balance of cropland cultivation of the region of Thessaly, Greece.*

	Mean	Std	Median	Q25	Q75
	[kt-N yr^{-1}]	[kt-N yr^{-1}]	[kt-N yr^{-1}]	[kt-N yr^{-1}]	[kt-N yr^{-1}]
N-Inputs	76.5	3.2	77.8	73.3	79.1
N-Outputs	71.7	3.2	71.2	69.4	73.7
N-stock-changes	4.8	0.0	6.6	3.9	5.4
Input fluxes					
N deposition	2.0	0.3	2.1	1.9	2.1
Bio. N fixation	16.7	1.6	16.7	15.9	17.5
N in min. fertilizer	28.9	1.7	29.3	27.6	29.8
N in organic fertilizer	28.9	1.3	29.2	27.9	29.8

Output fluxes					
Gaseous emissions[1]	21.2	3.1	21.1	18.9	23.4
N_2O	0.9	0.3	0.9	0.7	1.1
NO	1.1	0.5	1.0	0.7	1.4
N_2	4.9	2.4	4.5	2.9	6.6
NH_3	14.3	2.6	13.5	12.5	15.6
Aquatic fluxes[2]					
NO_3 leaching	3.9	1.3	3.8	3.0	4.7

1228   *1) Gaseous emissions are the sum of N2O, NO, N2 and NH3 fluxes; 2) Aquatic flux is nitrate leaching (NO3-)*

1229

1230   *Table A 5. Total crop yields per cultivar and year.*

Crop Yields [tons dry matter]					
Crops	2012	2013	2014	2015	2016	Mean
Cotton	303 676.9	374 424.6	359 806.7	322 292.0	285 780.3	329 196.1
Clover	302 753.2	319 401.7	338 134.6	341 938.4	360 693.9	332 584.4
Wheat	477 700.7	461 875.5	395 902.1	430 014.4	450 254.3	443 149.4
Barley	84 520.8	99 091.8	139 402.9	139 990.8	102 454.7	113 092.2
Maize	332 531.6	431 324.6	377 783.9	351 285.4	334 277.7	365 440.6

1231
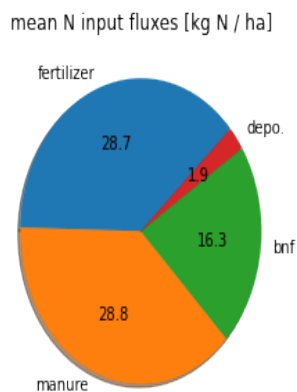
1232

1233   *Figure 9. Shares of components of the annual nitrogen in- and output fluxes.*

1234

1235   *Table A 6. Simulated crop yields per cultivar and year for the irrigated land.*

Crop Yields [tons dry matter ha^{-1}]

Crops	Median	Mean	STD
Cotton	4.0	3.7	0.9
Clover	9.8	9.6	0.6
Wheat	3.9	3.6	0.9
Barley	5.3	5.0	1.2
Maize	10.9	10.6	1.3

1236

1237 *Table A 7. Simulated crop yields per cultivar and year for the rain feed land.*

Crop Yields [tons dry matter ha^{-1}]			
Crops	Median	Mean	STD
Cotton	3.0	2.9	0.7
Clover	9.8	9.6	0.6
Wheat	3.9	3.6	0.9
Barley	4.0	3.9	0.9
Maize	9.5	9.2	1.5

1238